

Mechanical Design of a Connecting Rod for an Internal Combustion Engine

*MAE 296A – Damage & Failure of Materials in
Mechanical Design*



Figure 1: Solidwork realistic 3D model of connecting rod.

Wilson Lam

Solomon Li

Instructor

N.M. Ghoniem

10/25/2013

1 ABSTRACT

The objective of this report is to design and analyze a connecting rod for a Toyota 1NR-FE 4-cylinder engine. The connecting rod is made of 4130 Steel annealed at 865°C and utilizes an I-beam shape for its column cross section. Load analysis is performed to determine the axial and transverse forces on the connecting rod using Matlab. Using the loads obtained, a preliminary design of the cross section geometry is made based on beam theory. CAD software is used to create a two-dimensional solid model based on the preliminary design. Finite element analysis is performed on the solid model to determine the stress distribution in the connecting rod during the combustion cycle, and to compare the maximum stress to the yield strength of the material. The maximum stress is found to be 305 MPa compared to the yield strength of 460 MPa and this gave a desired safety factor of 1.5 when pocket thickness is at 0.007915m. Using 4130 Steel, the connecting rod lasts infinite fatigue life, withstanding 8.33×10^6 Engine Stress Cycles and 200,000 miles. As for fracture, using Mode I with a crack size below 0.2mm when manufactured, the connecting rod survives for infinite cycles.

Table of Contents

1	Abstract	1
2	List of Symbols	3
3	List of Figures	4
4	List of Tables	5
5	Introduction.....	6
6	Load Analysis	8
7	Engine Assumptions & Operating Loads.....	11
8	Beam Theory Analysis	13
9	Geometric Modeling and CAD	18
10	Finite Element Analysis & 2D Design Optimization	21
11	Fatigue/Lifetime Analysis	25
11.1	Steel 4310 test material	25
11.2	Al 1060 Alloy test material	27
12	Fracture Analysis.....	28
13	Solidworks and Abaqus 3D Design Optimization.....	31
14	Discussion & Conclusions	37
15	Summary and Conclusions	38
16	Acknowledgements.....	39
17	References	40
18	Appendices.....	41
18.1	Kinematic Equations Derivations	41
18.2	Force Components in the Inertial Reference Frame derivations	42
18.3	Materials Properties.....	44
18.4	TOYOTA AURIS TECHNICAL SPECIFICATIONS	46
18.5	N_f cycle vs. Edge Crack Size Matlab Code	48

2 LIST OF SYMBOLS

<i>Symbols</i>	<i>Descriptions</i>	<i>Units</i>
A	Area of piston	m^2
ω	Angular speed	rev/min
P	Axial force	N
b	Base length	m
A_x	Beam cross section area	m^2
h	Beam height	m
b	Beam thickness	m
M	Bending moment	Nm
r	Circle of radius crankshaft moves on	m
$P(\theta)$	Combustion pressure as a function of crank angle	Pa
γ	Connecting rod angle	$^\circ$
β	Connecting rod center of mass distance	m
G	Connecting rod center of mass vector	<i>Unitless</i>
ℓ	Connecting rod length	m
θ	Crank angle	$^\circ$
R	Crank vector	<i>Unitless</i>
Φ_{SR}	Force crankshaft exerts on connecting rod	N
Φ_{PR}	Force piston exerts on connecting rod	N
g	Gravitational Acceleration	m/s^2
m_G	Mass of connecting rod	Kg
m_P	Mass of piston	Kg
J_G	Moment of inertia of connecting rod about its center of mass	m^4
P	Piston vector	<i>Unitless</i>
λ	Ratio of crank length to connecting rod	<i>Unitless</i>
σ	Stress	N/m^2
T	Torque	Nm
S_y	Yield strength	N/m^2
E	Young's modulus	N/m^2
SF	Safety Factor	<i>unitless</i>
P_{cr}	Critical Stress	MPa
N	Cycles to Failure subscript(e-endurance & y-yield)	<i>unitless</i>
b_a	Axial body force	N/m^3
b_t	Transverse body force	N/m^3

3 LIST OF FIGURES

Figure 1: Solidwork realistic 3D model of connecting rod.	i
Figure 2: Diagram of location of acting forces and force component.	8
Figure 3: Engine Combustion Pressure vs. Crank Angle	10
Figure 4: (a) Left: Axial Force vs. Crank Angle (b) Right: Transverse Force vs. Crank Angle	10
Figure 5: (a) Left: Toyota 1NR-FE 4-cylinder engine [4] and (b) Right: Simplify schematic for engine assembly [3].	12
Figure 6: Connecting rod cross section design (a) rectangular (b) “T” beam.	14
Figure 7: Connecting rod cross section design in MATLAB.	15
Figure 8: Forces, axial load, and bending moment.	17
Figure 9: Front plane 2-D sketch with dimension.....	19
Figure 10: Extrude of the sketch.....	19
Figure 11: Mirror image and fillet corner to reduce stress concentration.	20
Figure 12: Final rendering in Solidworks 360 Photoview.....	21
Figure 13: Von Mises Stress analysis in Comsol (left) Deformation Scale: 50 (right) Deformation Scale: 500.....	22
Figure 14: Von Mises Stress analysis in Comsol (Deformation Scale: 1)(-6.28 rad).	23
Figure 15: Von Mises Stress analysis in Comsol (Deformation Scale: 1)(0 rad). ...	23
Figure 16: MAX Von Mises Stress analysis in Comsol (Deformation Scale: 1)(0.314 rad).	24
Figure 17: Von Mises Stress analysis in Comsol (Deformation Scale:1)(0.628 rad).	24
Figure 18: Single Cycle Damage Parameter (Green: significantly below 10^{-6})	26
Figure 19: Single Cycle Damage Parameter	28
Figure 20: Red is section of beam where crack appear.	29
Figure 21: Stress Cycle N_f vs. Edge Crack Size.....	30
Figure 22: (Top) Pocket depth: 0.003175m (Middle) Optimized (Bottom) Pocket depth: 0.009525.....	33
Figure 23: Tensile Stress at: (Top) Pocket depth: .007515 m (Bottom) Optimized Pocket depth: 0.007915m.....	34
Figure 24: Tensile Stress at Pocket depth: 0.008115m.....	35
Figure 25: Compressive Stress at Pocket size: 0.007915m.	36
Figure 26: Material properties of the connecting rod.....	44
Figure 27: Failed material properties of the connecting rod.	45

4 LIST OF TABLES

Table 1: Forces type	9
Table 2: Engine Specifications	12
Table 3: Engine operation assumption	12
Table 4: Material properties of the connecting rod (details in Appendix).....	15
Table 5: Beam theory assumption.....	16
Table 6: Max stress and safety factor.	17
Table 7: Force application and boundary conditions table.	22
Table 8: Stress vs. Pressure Profile angle.	25
Table 9: Steel 4130 annealed Connecting Rod S-N data.....	26
Table 10: Mileages and Number of Engine Cycles Data.....	27
Table 11: Al 1060 Alloy Connecting Rod S-N data.....	28
Table 12: Assumed crack properties for Steel 4130 [6].....	30
Table 13: Solidworks optimization data (For all the Stress plot look below).....	31
Table 14: Force application and boundary conditions table (Solidworks is applied in a similar so not listed here).....	32

5 INTRODUCTION

Connecting rods are used to convert rotational motion to linear reciprocating motion or vice versa. The typical use for connecting rods today are in internal combustion car engines, connecting the piston to the crankshaft and rotating it as the piston moves to the top and bottom of its stroke. The shape, geometry, and material of the connecting rod is extremely important to its performance and reliability [1].

Variations of connecting rod designs can include “I” beam and “H” beam. The “I” beam design offers good tensile strength while being able to withstand high compressive loads. This design is very commonly used in production engines, especially those with high rpm. In addition to the “I” beam design, another alternative is the “H” beam design, which is very stiff and can handle higher compressive loads than the “I” beam design. “H” beams are usually lighter and used in engines with low rpm range [2].

In addition to connecting rod geometry, the material used also rods plays a significant role on the mechanical properties. Connecting rods are made using various metals such as aluminum, steel, and titanium. Steel connecting rods are the most common due to its high strength and long fatigue life. However, using steel also adds more weight which requires more power from the engine. Another option are aluminum connecting rods which can be significantly lighter than steel connecting rods without jeopardizing strength. The reduction in weight allows the engine to rev faster and reduce vibration and stress on the crankshaft. Lastly, titanium connecting rods are another alternative because they are both lighter and stronger than steel, but come at a very costly price [2].

The main objective of this report is to design a connecting rod for an economy-sized sedan. The initial part of the design process includes load analysis and beam theory. The objective of this phase is to determine the loads acting on the

connecting rod which are later used as inputs to finite element analysis, and to determine rough initial dimensions for the connecting rod cross section. Finite element analysis is done to find the maximum stress and its relation to the material yield strength. Also, fatigue and fracture analysis are performed to further optimize the mechanical properties of the connecting rod. With this information, a three-dimensional solid model of the connecting rod with the desired material and geometry can be made using Solidworks and Abaqus.

To work towards these objectives, load analysis on the connecting rod will be done first. Loads including the contact force from the crankshaft, contact force from the piston, and inertial forces due to dynamic motion will be determined. These loads will be used to calculate rough initial dimensions of the cross section of the connecting rod using beam theory. Also using this data, the maximum stress in the beam and safety factors against yield and buckling will be determined. A two-dimensional solid model for finite element analysis will be made in CAD using the cross section dimensions obtained. Then, finite element analysis will be performed on the connecting rod to find the stress distribution in the connecting rod during the combustion cycle and compare to the yield strength of the material. Furthermore, finite element analysis is performed to evaluate the effects of fatigue and fracture on the connecting rod. Revisions on the dimensions will be made on the two-dimensional solid model accordingly until the optimal design is reached. Finally, a three-dimensional solid model will be made using Solidworks and undergo three-dimensional elastic finite element analysis using Abaqus.

In the following report, the load analysis of the connecting rod is presented first, followed by the engine assumptions and operating conditions, preliminary design using beam theory, two-dimensional solid model, two-dimensional elastic finite element analysis, fatigue analysis, fracture analysis, Abaqus three-dimensional design optimization, discussions & conclusions, and finally the summary.

6 LOAD ANALYSIS

In this section, the objective is to determine and analyze the various internal and external forces acting on the connecting rod through fundamental load analysis. After obtaining the necessary forces, these values will be used to later perform Finite Element Analysis (FEA) and optimize the connecting rod design for durability, strength, and weight.

Before analysis of the connecting rod, certain assumptions must be made on the forces acting on the connecting rod.

The assumptions are the following forces acting on specific locations during constant angular speed:

- External force acting only from pin location:
 - o Contact force from the piston
 - o Contact force from the crankshaft
- Inertial force due to its motion

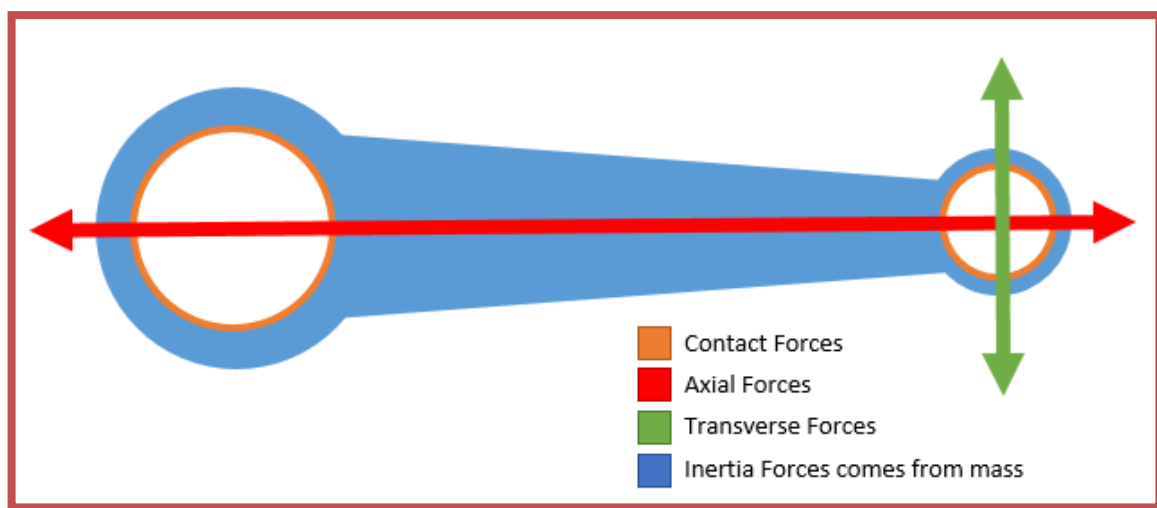


Figure 2: Diagram of location of acting forces and force component.

Table 1: Forces type

Type of Forces	Descriptions
Contact Forces	Forces acting at contact location: - Piston - crankshaft
Inertia Forces	Forces acting on accelerated object
Axial Forces	Decomposed force from resultant force
Transverse Forces	Perpendicular to Axial force

The kinematic equations to obtain the following graphs are (refer to Figure 5b for a schematic diagram) listed below:

$$\text{Eq 6-1} \quad \mathbf{R} = -r \sin\varphi (i) + r \cos\varphi (j)$$

$$\text{Eq 6-2} \quad \mathbf{P} = (r \cos\varphi - l \cos\gamma) = l(\lambda \cos\varphi - \cos\gamma)(j)$$

$$\text{Eq 6-3} \quad \mathbf{P} = \mathbf{R} + \beta(\mathbf{P} - \mathbf{R}) = (1 - \beta)\mathbf{R} + \beta\mathbf{P}$$

$$\text{Eq 6-4} \quad m_p \ddot{\mathbf{P}} = -p(\varphi)A(j) - \Phi_{PR} + \Phi_{CP}(i)$$

$$\text{Eq 6-5} \quad m_G \ddot{\mathbf{G}} = \Phi_{PR} + \Phi_{SR}$$

$$\text{Eq 6-6} \quad J_G \ddot{\gamma}(k) = \Phi_{PR} \times (\mathbf{G} - \mathbf{P}) + \Phi_{SR} \times (\mathbf{G} - \mathbf{R})$$

For the derivation of the rest of the kinematic equations used in the Matlab code, refer to the Appendix.

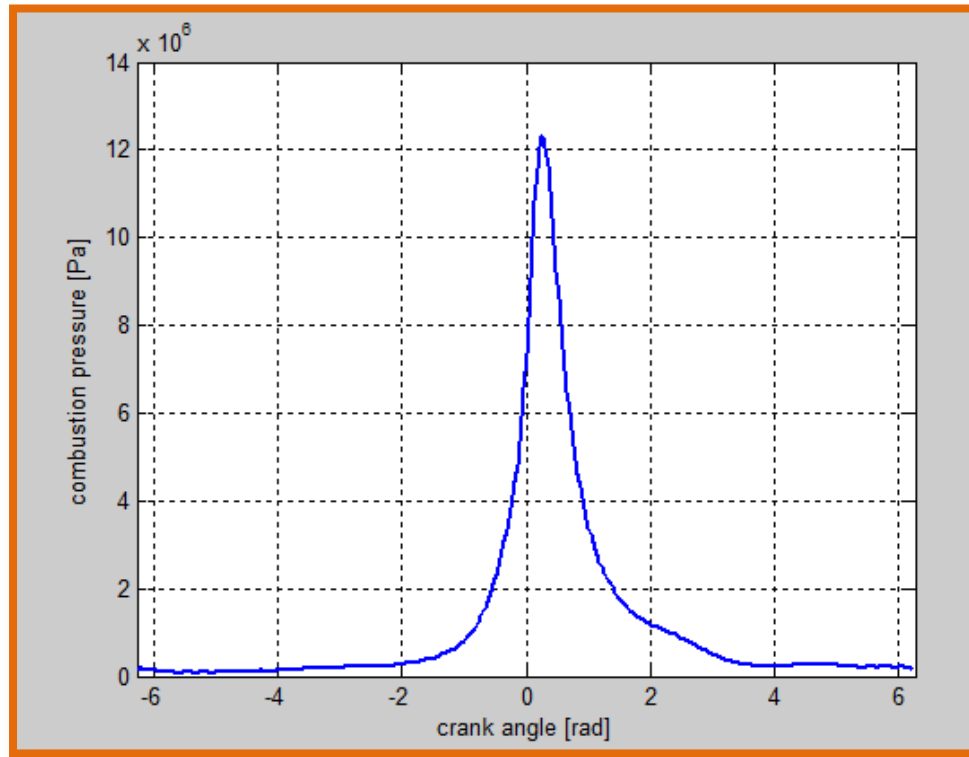


Figure 3: Engine Combustion Pressure vs. Crank Angle

Figure 3 is based on provided combustion pressure data acting on a piston during a 5000 rpm cycle. The axial force and transverse forces are also determined from the combustion pressure as well.

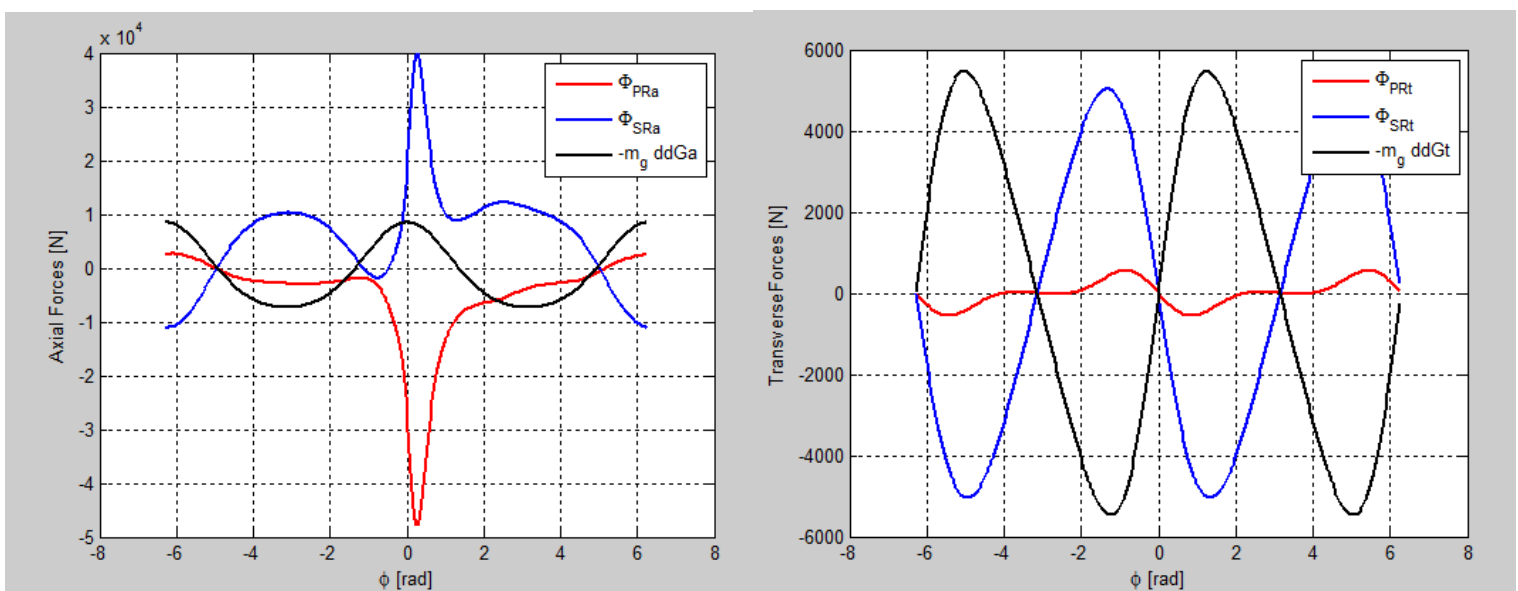


Figure 4: (a) Left: Axial Force vs. Crank Angle (b) Right: Transverse Force vs. Crank Angle

The following axial force and transverse force calculated are the forces transferred to the connecting rod. The calculations for these forces are shown in the Appendix.

The maximum force for the axial force is between 0 to 0.4 rad when the Φ_{SRa} and Φ_{PRa} peaks in Figure 4(a). The transverse force Φ_{SRt} and Φ_{PRt} peaks around -5, -1, 1, and 5 radian. From this analysis, we know that when performing Comsol analysis later, we should carefully analyze the stress when the pressure profile is around 0-0.4 rad for peak stress when axial force is maximum.

Since the analysis is done during constant angular speed of the connecting rod, all forces are assumed to be periodic during each combustion cycle. During the motion these forces are expected to create tension, compression, stress, shear, and moment on the connecting rod. These forces will help determine the stress and moment necessary to fracture the connecting rod. The experimental data will be used to determine the critical load based on material stress properties, and determine a safety factor to prevent possible failure of the connecting rod during its lifetime operation.

7 ENGINE ASSUMPTIONS & OPERATING LOADS

The engine used in this analysis is based off a Toyota 1NR-FE inline 4-cylinder engine. This means that the engine operates similar to the design of the Matlab code and has the following schematic below.

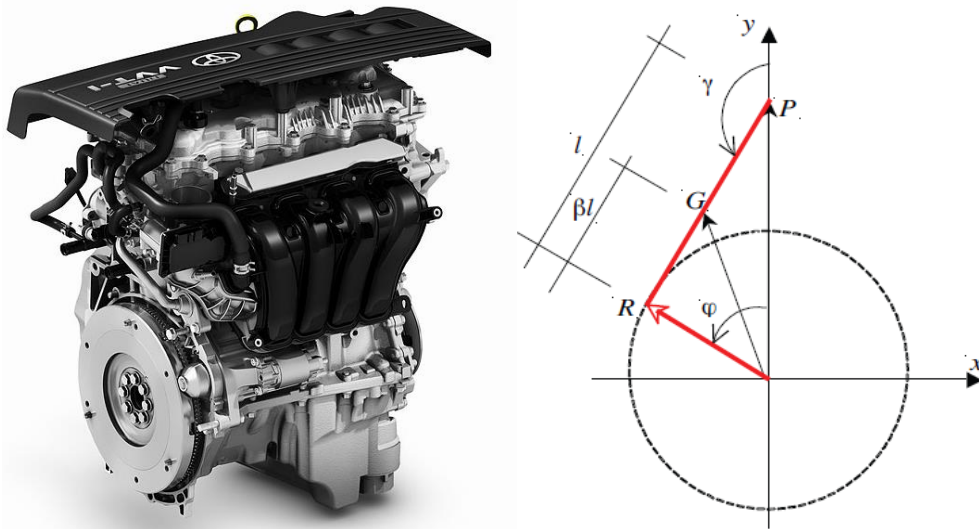


Figure 5: (a) Left: Toyota 1NR-FE 4-cylinder engine [4] and (b) Right: Simplify schematic for engine assembly [3].

Table 2: Engine Specifications

Engine	1.33L Dual VVT-i
Engine Code	1NR-FE
Displacement	1,329cc
Power	101hp @ 6,000 rpm
Torque	132Nm @ 3,800 rpm
Bore	72.5 mm
Stroke	80.5 mm
Compression	11.5:1
Combined economy	48.7 mpg
CO ₂ emissions	135 g/km

In this section, engine data will be taken from Table 2. Even with the data, certain assumptions are still made. These assumption and values are later used in the Matlab code to create the necessary Force vs. crank angle plots.

Table 3: Engine operation assumption

Assumption Engine	1.33L Dual VVT-i
Piston Mass	0.42 kg
RPM	3,800 rpm
Expected Torque	132 Nm

The engine is assumed to be operating at a constant 3,800 rpm because there was insufficient engine data for other operating speed. All data is based off the operating speed at 3,800 rpm. Further results obtaining the following data and equations necessary for the experimental result are in the Appendix.

The next assumption is on the combustion pressure profile $p(\theta)$. This pressure is assumed to be known at a constant ω and is provided from another data source. The data source is specifically for a 5000 rpm operation cycle so this will change the experiment outcome from the true outcome for an engine operating at 3,800 rpm. After inputting these parameters the data can be used to measure the axial load and bending moment in the next section.

8 BEAM THEORY ANALYSIS

This section will explain the idealizations performed on the connecting rod to simplify the calculation without compromising the results. The section that will be focused is the center of the connecting rod as shown below.

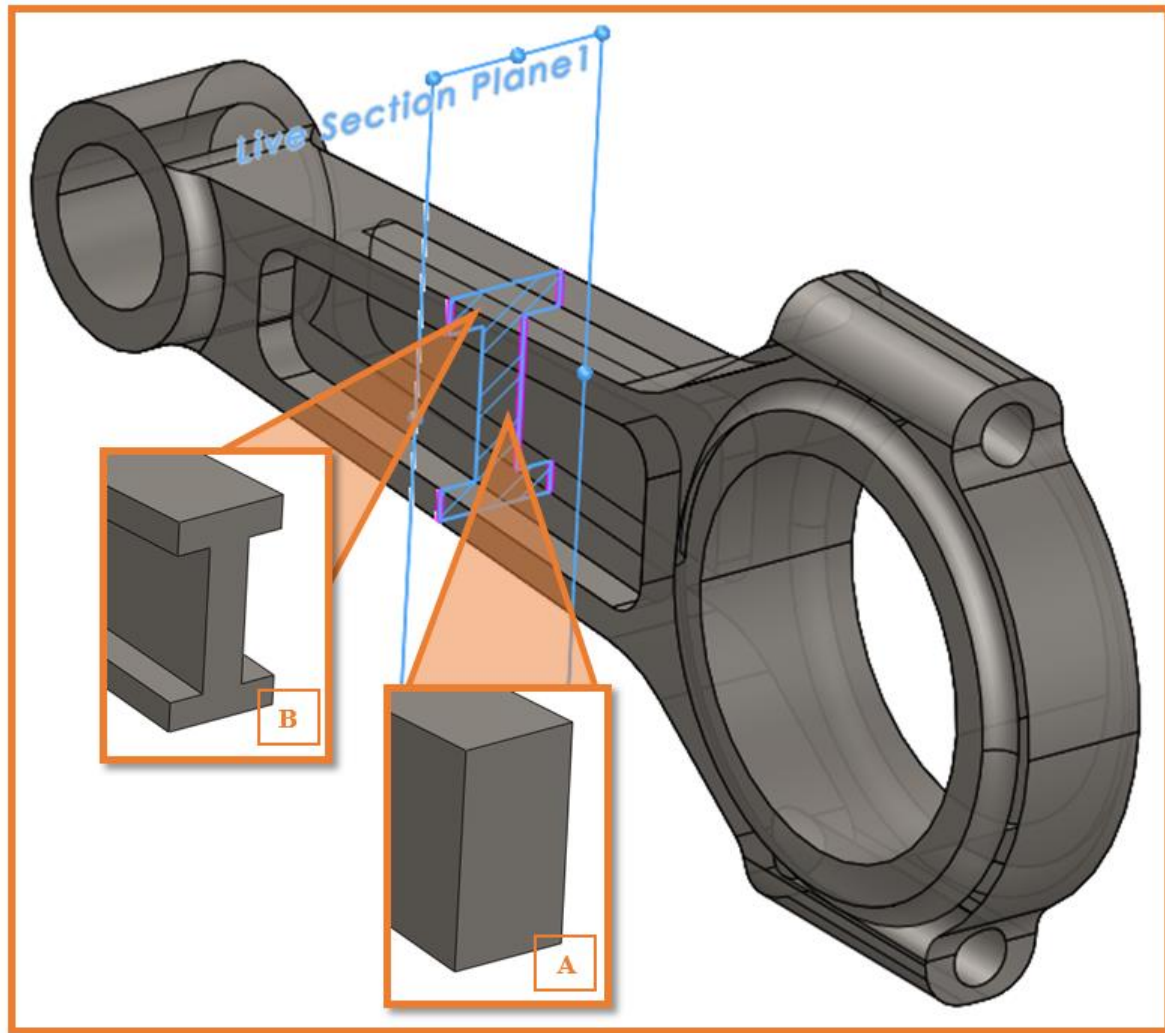


Figure 6: Connecting rod cross section design (a) rectangular (b) “T” beam.

For the connecting rod, it was initially designed to have a rectangular cross-section and the preliminary analysis for the MATLAB code is done using this design. The diagram above shows the type of cross section that will be analyzed in this study. The I-beam will later be used in the optimization analysis to better improve the connecting rod performance. For now, the analysis is done on a rectangular cross-section.

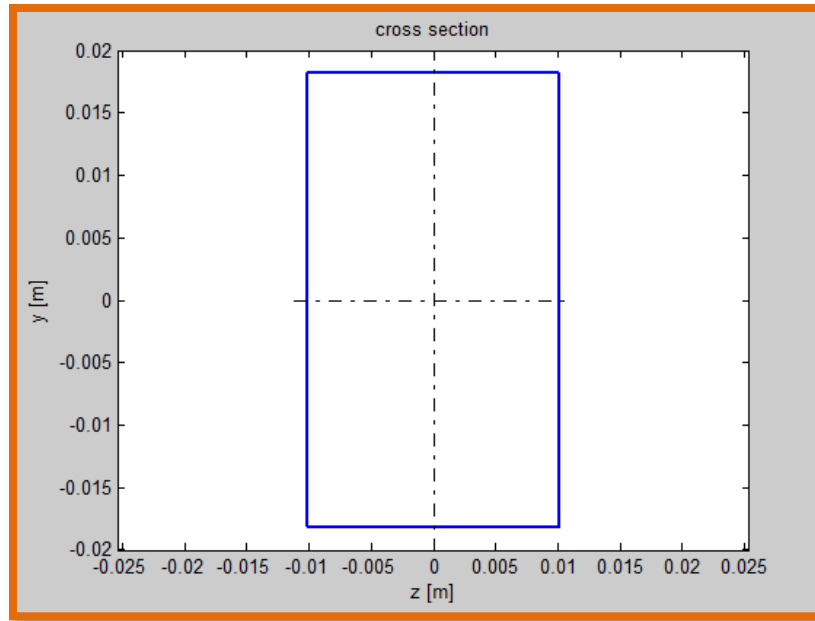


Figure 7: Connecting rod cross section design in MATLAB.

The materials we used for the connecting rod is listed below.

Table 4: Material properties of the connecting rod (details in Appendix).

Material Properties	
Elastic Modulus	205 GPa
0.285Poisson's Ratio	0.285
Shear Modulus	80 GPa
Density	7850 kg/m ³
Tensile Strength	560 MPa
Yield Strength	460 MPa

To calculate for the rectangular cross-section, we first have to find the moment of inertia using the equation below:

$$\text{Eq 8-1} \quad I_1 = \frac{bh^3}{12}$$

For an I-beam, the parallel axis theorem is used to calculate for the sectioned rectangular pieces.

$$\text{Eq 8-2} \quad I_2 = I + Ad^2$$

Summing the sectioned moment of inertia we would get the total moment of inertia.

After obtaining Φ_{SR} and Φ_{PR} (forces) as well as its individual x and y components, Figure 4 in terms of crank angle is plotted. Now we will use these forces to obtain load and moment. The equations to calculate for the stress are:

$$\text{Eq 8-3} \quad \sigma_x(x, y, \phi) = \frac{P(x, \phi)}{A_x} - \frac{M(x, \phi)y}{I_z}$$

The moment of inertia I_z can be calculated with respect to the cross-sectional area related to z-axis and cross-section area A_x as shown in Figure 6. But to determine the maximum axial stress, the following equation is used.

$$\text{Eq 8-4} \quad \sigma_x(x, \phi)_y = \frac{|P(x, \phi)|}{A} + \frac{|M(x, \phi)y|}{2I_z}$$

With the equation above we can now obtain the max axial stress.

Table 5: Beam theory assumption.

Terms	Values
Cross section Height	0.0364 m
Cross section Length	0.0203 m
Moment of Inertia (connecting rod at center of mass)	0.00655 m ⁴
Center of Mass (CM) (from large pinhole center)	56 mm
Connecting Rod length (CRL) (pinhole to pinhole)	178 mm
Beta = CM/CRL	0.315 unitless
Moment of Inertia of Cross Section	$I_y = 2.5 \times 10^{-8} \text{ m}^4$ $I_z = 8.2 \times 10^{-8} \text{ m}^4$
Material Properties	4130 Steel annealed at 865°C
Young's Modulus (E)	$2.05 \times 10^{11} \text{ Pa}$
Yield Strength (S_y)	460 MPa

With all the following data to input into the “Load_Analysis.m” and “Beam_Analysis_01.m,” the axial load and bending moment were obtained[4].

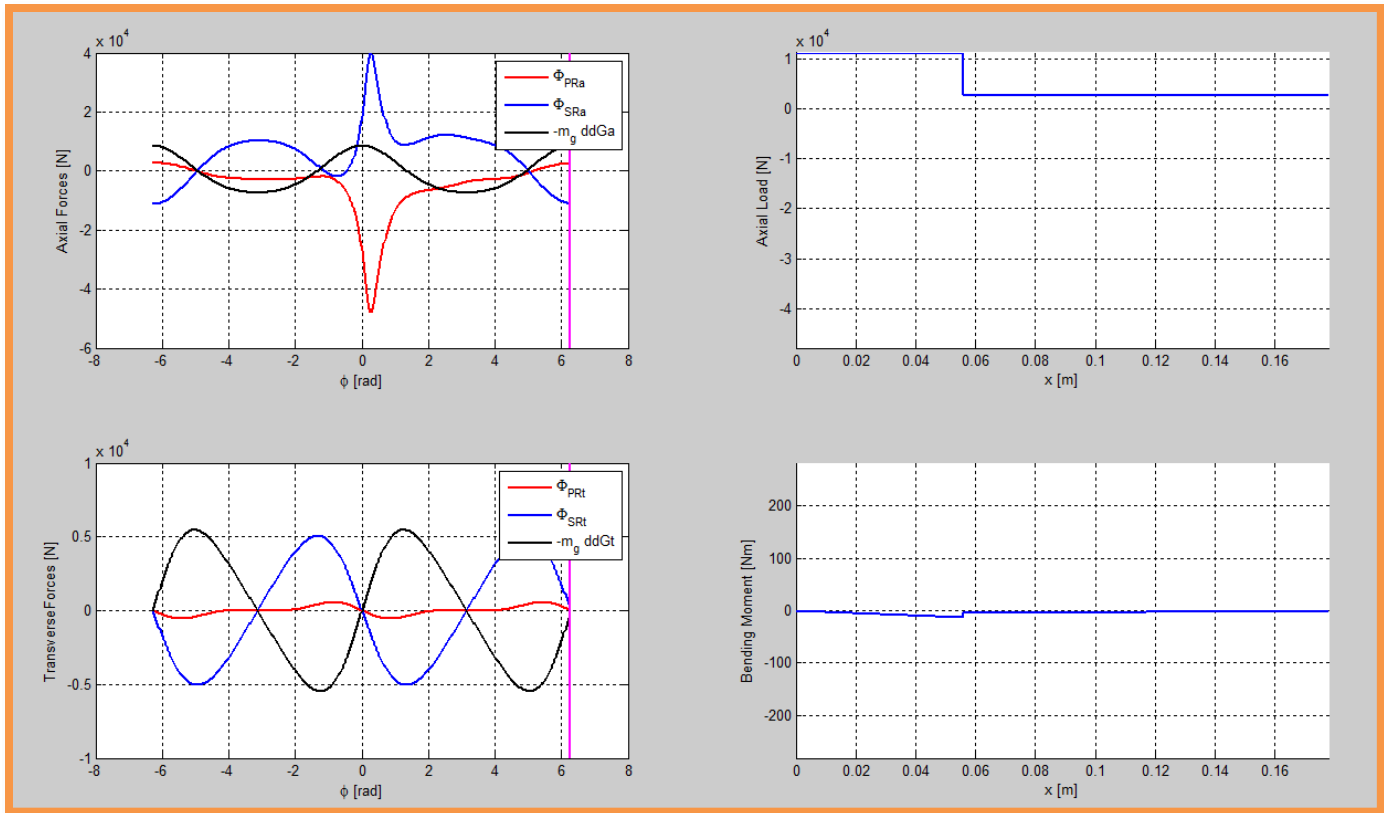


Figure 8: Forces, axial load, and bending moment.

The axial load and moment is now obtained. With the stress equation above and the following equations below, the following data can be determined.

Table 6: Max stress and safety factor.

Description	Values
σ_{max}	77.1 MPa
yield safety factor	5.9689
Pcr z	3.32 MPa
buckling z safety factor	299.1303
Pcr y	1.04 MPa
buckling y safety factor	93.2975

To determine the values above the following equations are used:

- This equation is use to determine the yield safety factor:

$$\text{Eq 8-5} \quad SF_{yield} = \frac{S_y}{\sigma_{max}}$$

- This equation is use to determine the $P_{cr@z}$ and $SF_{buckling-z}$:

$$\text{Eq 8-6} \quad P_{cr@z} = \frac{2\pi EI_z}{l^2}$$

$$\text{Eq 8-7} \quad SF_{\text{buckling-z}} = \frac{P_{\text{cr@z}}}{P_{x-\text{max}}}$$

- This equation is use to determine the $P_{\text{cr@y}}$ and $SF_{\text{buckling-z}}$:

$$\text{Eq 8-8} \quad P_{\text{cr@y}} = \frac{2\pi EI_y}{l^2}$$

$$\text{Eq 8-9} \quad SF_{\text{buckling-z}} = \frac{P_{\text{cr@y}}}{P_{x-\text{max}}}$$

As shown in Table 6, the various safety factors are determined for the connecting rod middle section. We had to perform a different analysis to obtain values for the circular region due to its complexity. In the later section FEA for the connecting rod will be done which will provide more data for comparison with these results. But since the Comsol and Abaqus will take the whole part into consideration and max stress is expected to occur in the thinner part of the connecting rod cross-section, the Comsol and Abaqus model is expected to have a lower factor of safety on this preliminary design.

9 GEOMETRIC MODELING AND CAD

The project utilized Solidworks to create a three-dimensional CAD model of the connecting rod. First, a two-dimensional sketch of the front plane of half the connecting rod is made on the Front Plane. The sketch is then labeled accordingly with the appropriate dimensions for the height, length, inner radius, outer radius, and other features. Next, the two-dimensional sketch is extruded to the appropriate width using Extrude Boss/Base, resulting in a three-dimensional model of half the connecting rod. Afterwards, additional features for the circles are sketched and extruded as well. Then, the other half of the connecting rod is formed by using the Mirror feature and more details are made to the model such as filleting the sharp corners and adding pockets to the connecting rod using the Fillet option. Finally, a photorender of the three-dimensional model is made using the Photoview 360 feature to give a realistic aesthetic look.



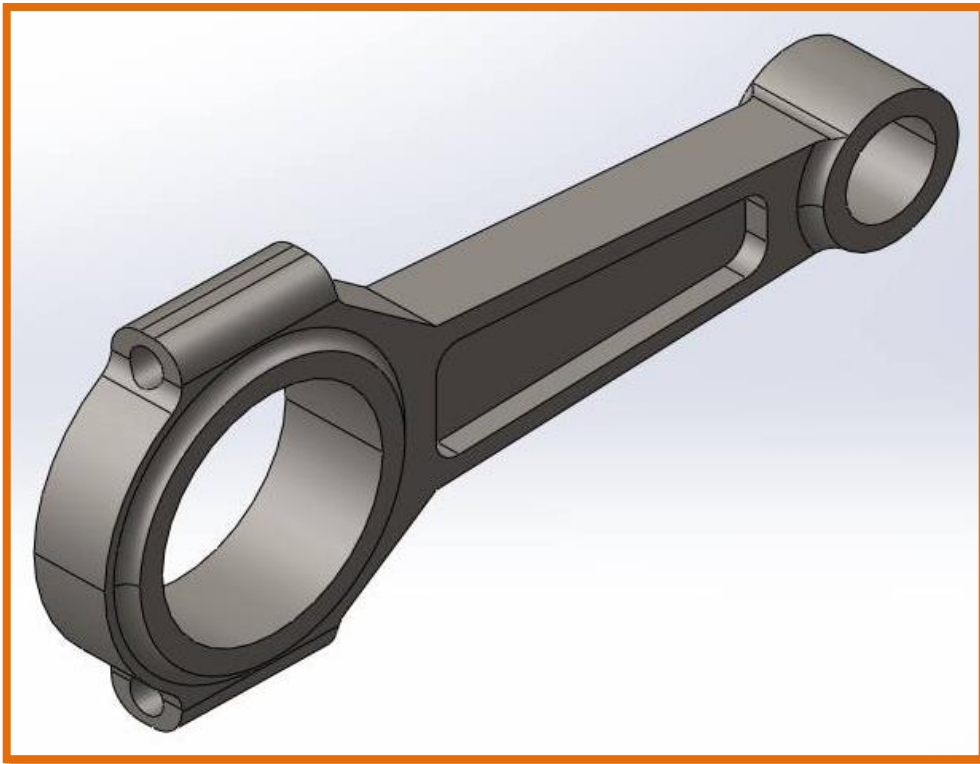


Figure 11: Mirror image and fillet corner to reduce stress concentration.



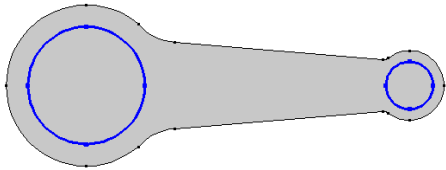
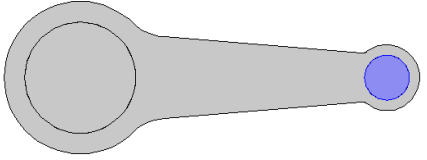
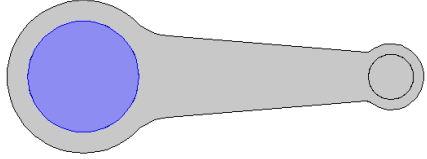
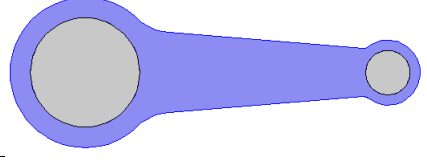
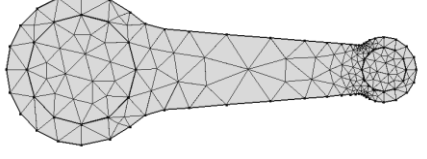
Figure 12: Final rendering in Solidworks 360 Photoview.

10 FINITE ELEMENT ANALYSIS & 2D DESIGN OPTIMIZATION

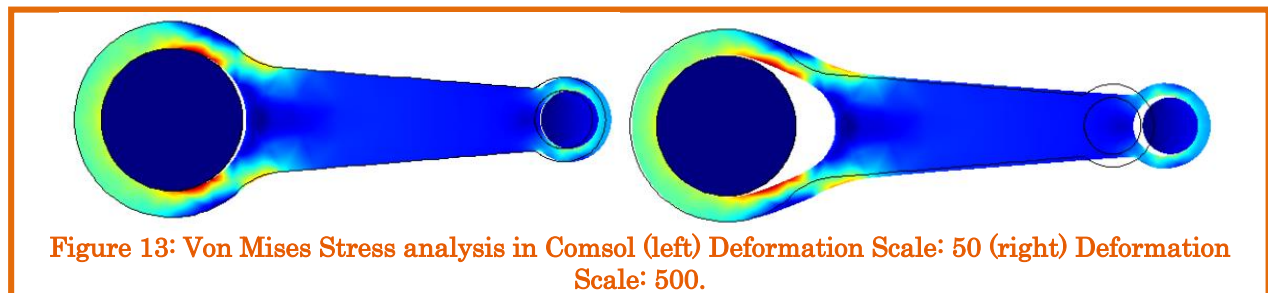
After obtaining all the results from MATLAB, analysis in Comsol is started. Plane stress analysis will be performed in Comsol. To do this, a 2D model similar to the Solidworks model used earlier is redesigned (displayed below).

After designing the 2D model and giving it a thickness, the next step is setting the boundary conditions. The load is based off of the pressure profile provided in order to perform the calculation [3]. The following setup below must be done before the Comsol is run. The following table below lists the force application and boundary conditions.

Table 7: Force application and boundary conditions table.

Conditions	Values
The following shows the boundary selections and also the contact locations that is related to the boundary conditions.	
Prescribed displacement: $Y = 0 \text{ m}$ Prescribed Body load: $X = \text{FPRa}$ $Y = 0 \text{ N}$	
Prescribed displacement fixed/anchored.	
Body load: $X = \text{ba N/m}^3$ $Y = \text{bt N/m}^3$	
Mesh size: Course Note: PC failed to run fine mesh or anything lower.	

Once the boundary conditions are prescribed, Comsol analysis can be used. The results of the FEA can be found below with a deformation scale of: 1, 50, and 500.



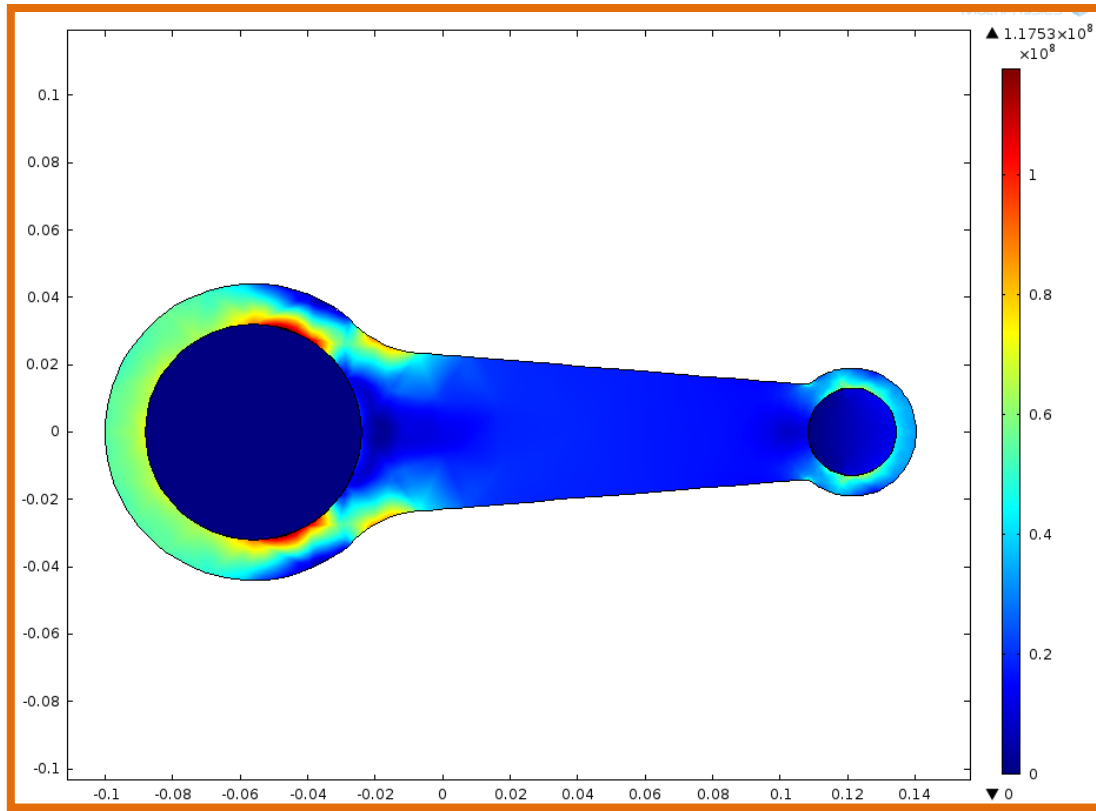


Figure 14: Von Mises Stress analysis in Comsol (Deformation Scale: 1)(-6.28 rad).

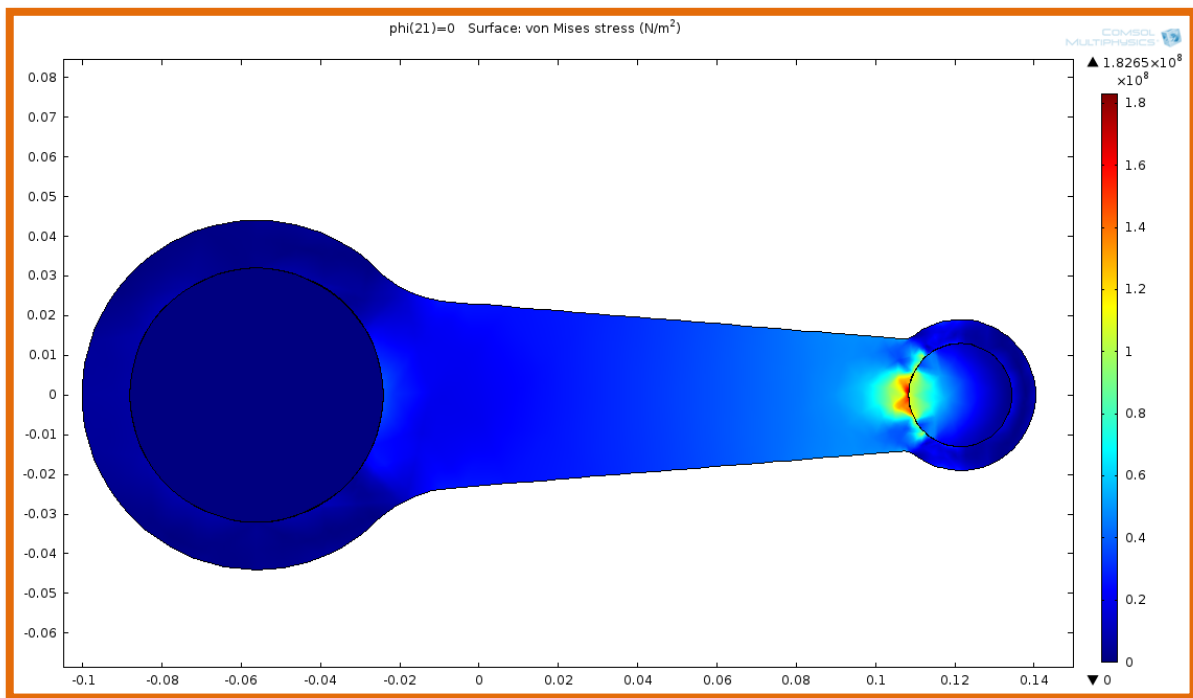


Figure 15: Von Mises Stress analysis in Comsol (Deformation Scale: 1)(0 rad).

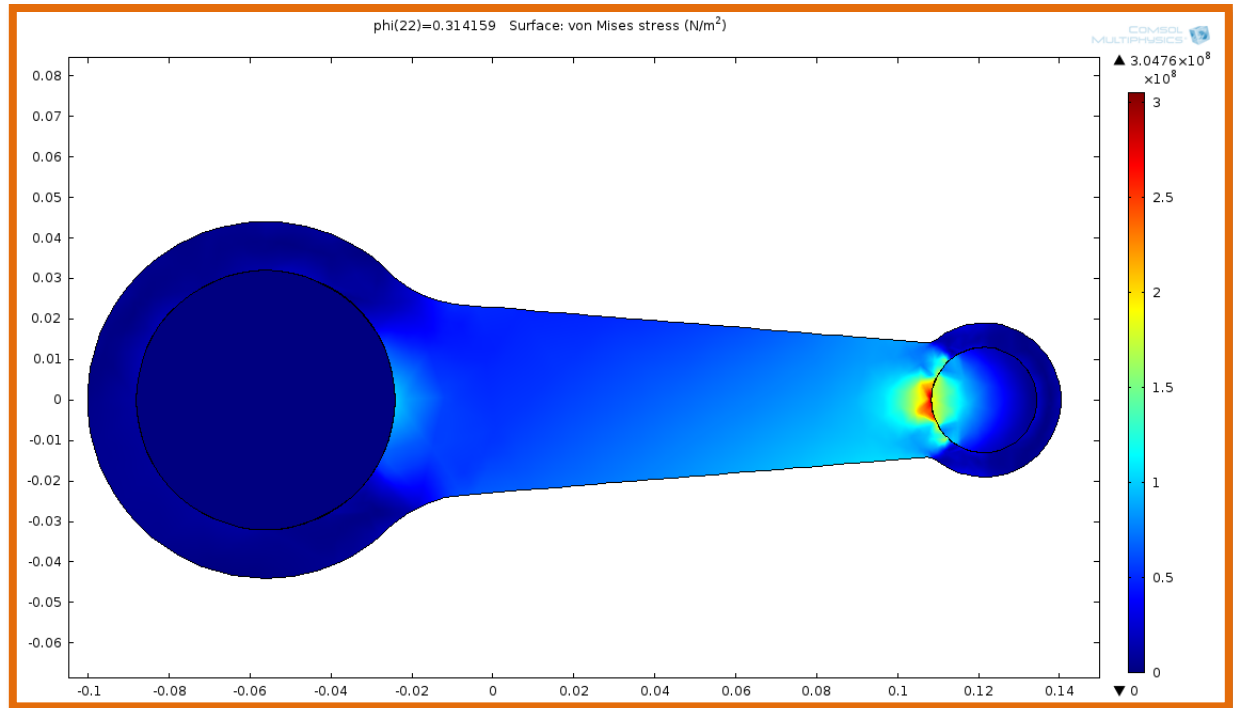


Figure 16: MAX Von Mises Stress analysis in Cmsol (Deformation Scale: 1)(0.314 rad).

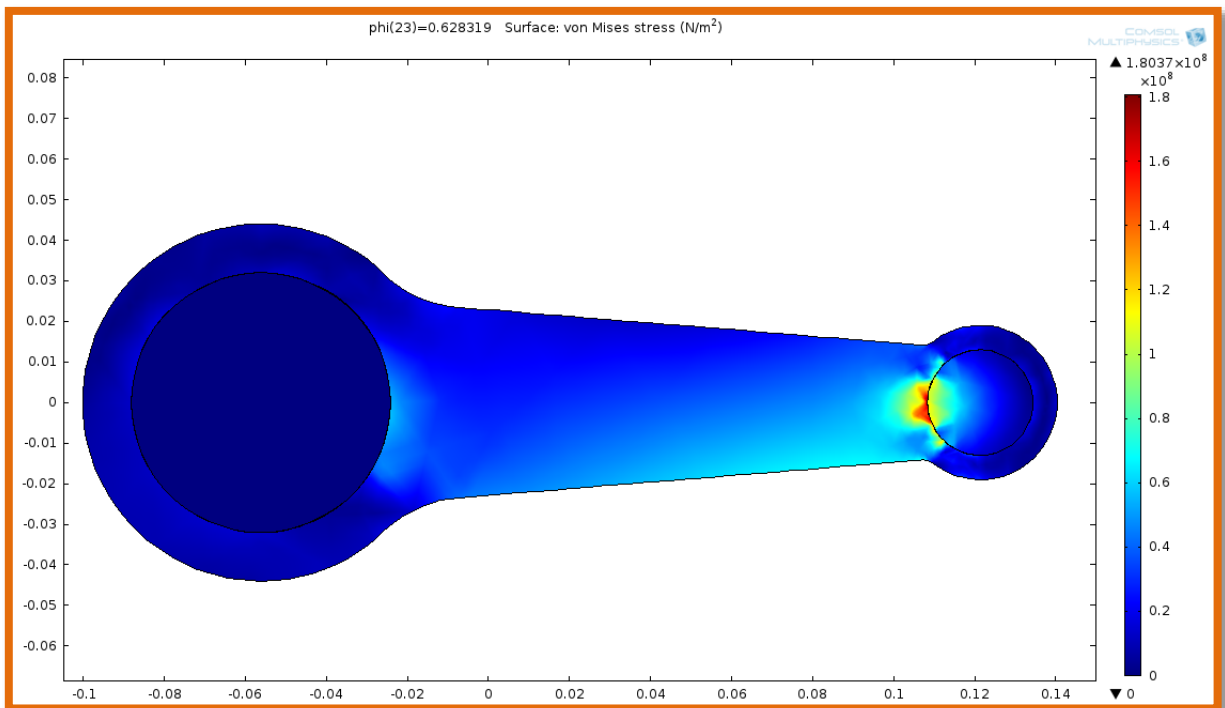


Figure 17: Von Mises Stress analysis in Cmsol (Deformation Scale:1)(0.628 rad).

Table 8: Stress vs. Pressure Profile angle.

Pressure Profile Angle (rad)	Stress (Pa)
-6.28	1.17×10^8
0	1.83×10^8
0.314	3.05×10^8
0.628	1.80×10^8

$$\text{Eq 10-1} \quad \text{COMSOL FOS} = \frac{S_y}{S_{\text{accepted failure}}} = \frac{460 \text{ MPa}}{305 \text{ MPa}} = 1.5$$

After performing the FEA, values from Table 8 were obtained. The maximum stress is at 305 MPa which is about 3/4 times the yield strength of 460 MPa, which gives a safety factor of 1.5. This means that our first analysis in Comsol showed that the primary material and design used in the FEA will survive the angular speed of 3800 RPM conditions.

From the figures of the FEA above, we can conclude that there is very minimum stress in the beam column. This means that in our final analysis we can change and vary the thickness of the middle column to reduce mass. This middle column as discussed earlier could be changed from a rectangular cross section to an I-beam. From using an I-beam design, we expect the mass to be lower and still be able to survive the stress test. Also, using the I-beam design, we expect to vary the thickness while maintaining an adequate safety factor for the cross section to survive. This is done in the last section.

11 FATIGUE/LIFETIME ANALYSIS

We will be performing tests on a few materials to see which one best fits our requirement for the connecting rod to survive infinite cycles. Although we test a few more materials we will only be comparing two materials below and identifying only the best material with affordable price (ex. titanium is too expensive).

11.1 *Steel 4310 test material*

A lifetime analysis is crucial in determining the lifetime operation of the Steel 4130 annealed connecting rod before failing. To do this test the material

properties must be known and an analysis on fatigue must be done. For fatigue type there are usually two common type low-cycle (strain-controlled) and high-cycle (stress-controlled). For the connecting rod we expect the analysis to be done using high-cycle because the connecting rod is expected to last a large number of cycles. This analysis is going to be performed using MATLAB and fatigue equations.

(Default Data: N_y and N_e are default values 100 and 10^6 respectively as this data are not available for public access.)

Table 9: Steel 4130 annealed Connecting Rod S-N data.

Cycle Type	Number of Cycles (unitless)
N_y (default data)	100
N_e (default data)	10^6
N_t	Infinite Over 10^6 (25,000 mi > 10^6 engine cycles)
Calculated N_{vehicle}	8.33×10^6

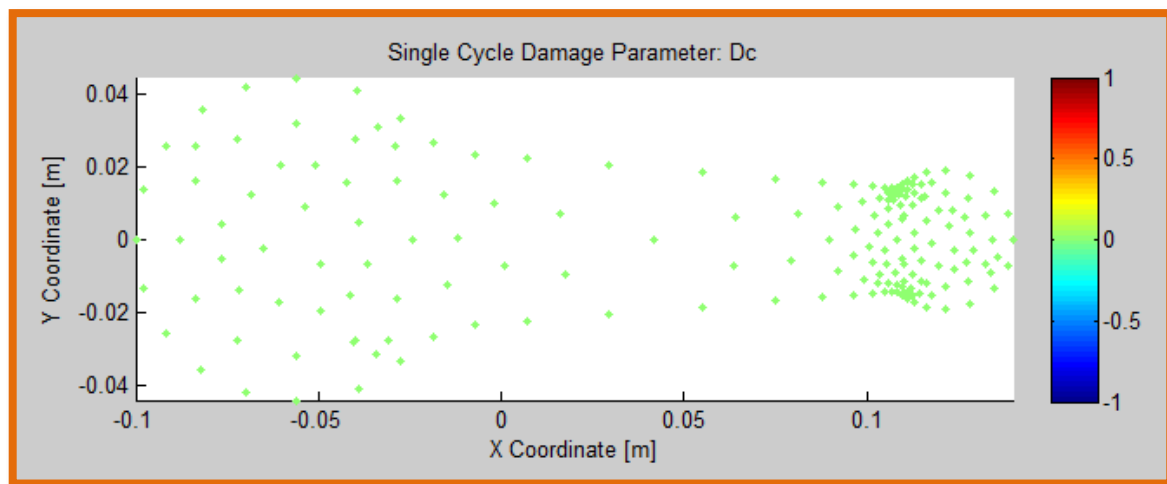


Figure 18: Single Cycle Damage Parameter (Green: significantly below 10^{-6})

Note: Figure 18 has fewer points because during Comsol analysis, finer mesh would not run due to PC capabilities (even if finer mesh is used results should not change the infinite life obtained).

The calculated N is in the infinite range (therefore Green) as expected since most cars now are designed to last an infinite cycle. The whole part is represented as green because it is in the infinite range and won't fail during the 200,000 miles

lifetime operation. That is the common norm as cars are lasting 200,000 miles easily. We estimate the vehicle to survive 200,000 miles and perform the calculation to obtain the desire lifetime stress N.

Wheel Diameter (D) = 0.762 m

Max Gear Ratio: 1st Gear * Differential Gear = 3.538(4.562) = 16.14

$$\text{Eq 11-1} \quad N_{\text{vehicle}} = 200,000 \text{ (miles)} * \frac{1609.34 \text{ (m)}}{1 \text{ (miles)}} * \frac{\text{Wheel cycles}}{\pi D \text{ (m)}} * \frac{\text{Engine cycles}}{16.14 \text{ Wheel Cycles}} =$$

$8.33 * 10^6 \text{ Engine Stress Cycles}$

Table 10: Mileages and Number of Engine Cycles Data.

Differential	Gear 1	Gear 2	Gear 3	Gear 4	Gear 5	Gear 6	Reverse
4.562	3.538	1.913	1.310	0.971	0.818	0.700	3.333
Car Mileages	Number of Engine Cycles (Each column relate to that particular gear)						
200000	8.33E+06	1.54E+07	2.25E+07	3.04E+07	3.60E+07	4.21E+07	8.84E+06
175000	7.29E+06	1.35E+07	1.97E+07	2.66E+07	3.15E+07	3.68E+07	7.74E+06
150000	6.25E+06	1.16E+07	1.69E+07	2.28E+07	2.70E+07	3.16E+07	6.63E+06
125000	5.21E+06	9.63E+06	1.41E+07	1.90E+07	2.25E+07	2.63E+07	5.53E+06
100000	4.17E+06	7.70E+06	1.12E+07	1.52E+07	1.80E+07	2.11E+07	4.42E+06
75000	3.12E+06	5.78E+06	8.44E+06	1.14E+07	1.35E+07	1.58E+07	3.32E+06
50000	2.08E+06	3.85E+06	5.62E+06	7.59E+06	9.01E+06	1.05E+07	2.21E+06
25000	1.04E+06	1.93E+06	2.81E+06	3.79E+06	4.50E+06	5.26E+06	1.11E+06

As expected, the $8.33 * 10^6 \text{ Engine Stress Cycles}$ is significantly over the N_e ; therefore, this qualifies as infinite life. This is also the main reason most connecting rods are made from this material because cost and fatigue life fits perfectly for operation. **Important:** the design of the connecting rod needs to have infinite life. If not, it will fail since at 25,000 miles from Table 10, the engine cycles already have over 10^6 cycles.

11.2 Al 1060 Alloy test material

(for reference to material above that Matlab Code is working properly)

In this experiment of Al 1060 alloy, the material is expected to fail very quickly due to low stress.

Table 11: Al 1060 Alloy Connecting Rod S-N data.

Cycle Type	Number of Cycles (unitless)
N_y (default data)	100
N_e (default data)	10^6
N_t	Infinite Over 10^6
Calculated N_{vehicle}	50

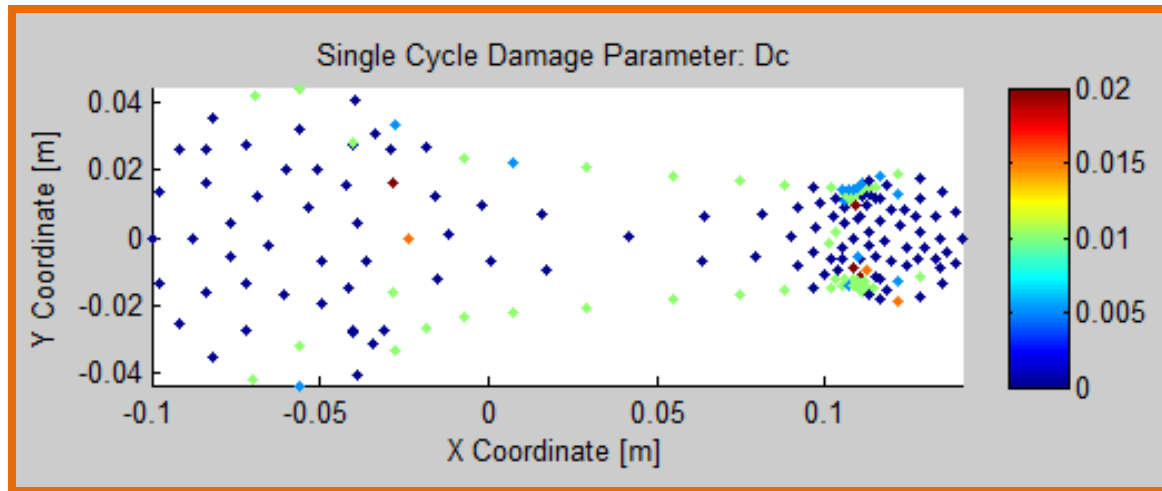


Figure 19: Single Cycle Damage Parameter

Note: Figure 19 has fewer points because during Comsol analysis finer mesh would not run due to PC capabilities (in this case finer mesh would provide better results, but we know this material will fail).

Using the same equations as above and Matlab code, Al 1060 alloy is chosen as the test material for fatigue analysis and it fails after only 50 engine stress cycles, which is equivalent to 3-4 wheel stress cycles.

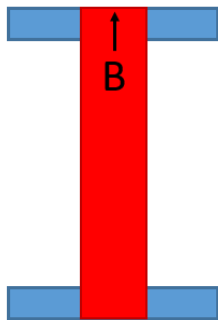
Again, materials used should be Steel 4130 or materials with equivalent strength and stress cycle. If not, the connecting rod will fail during low engine operation cycles and will not last the desired 200,000 miles lifetime. Thus this is one major reason why steel was chosen. Although some types of Aluminum are a lot stronger, they are often more costly.

12 FRACTURE ANALYSIS

When designing a connecting rod, fracture from cracks must be considered to determine when the connecting rod might fail. When doing this analysis, the connecting rod is assumed to be under linear elastic fracture mechanics (LEFM) conditions.

Our assumptions are as follows:

- Crack start from edge (under tension crack usually start at edge)
- Beam section is rectangle
- But cross-section area is base off the thinnest part of I-beam
(Reduce the I-beam to rectangular beam for simplicity red part in diagram below.)



In this analysis, the crack is assumed to start at the red section where there is less material for it to travel through.

- $2h = 0.107569$ m (into the page)
- $b = .006$ to $.01397$ m ($a = .0005$ m) [$a/b = 0.036$ to $0.083 < 0.1$ so $\beta \leq 1.2$]

In any case, the crack length “a” is expected to be less than 0.5mm. If not, it is a completely visible crack. This gives an approximate $\beta = 1.0$ to 1.2. As long as the initial crack size a/b ratio is below 0.1, $\beta = 1.2$ can be used as a constant and does not vary much with crack size “a”. (Note: all stress concentration converges to 1 as crack becomes smaller.)

Figure 20: Red is section of beam where crack appear.

The crack size is below .0005m because normally crack sizes are not visible to the human eye and anything above this value is visible.

The crack growth rate is assumed to give the following equations and by Paris Law [6]

$$\text{Eq 12-1} \quad \frac{da}{dN} = C(\Delta K_I)^m \text{ (Paris Law)}$$

$$\text{Eq 12-2} \quad \Delta K_I = \beta \Delta \sigma \sqrt{\pi a}$$

Combining Eq 12-1 and Eq 12-2, they can be integrated and solved for N stress cycle (Stress are obtain from the Comsol Analysis).

Table 12: Assumed crack properties for Steel 4130 [6].

Constants/Variable	Material Constant/Value
C	$6.89 \times 10^{-12} \text{ (m/cycle)/}(\text{MPa}\sqrt{\text{m}})^m$
m	3.00 unitless
β	1.2
N_f (edge crack size: <0.2mm)	$\sim 10^6$

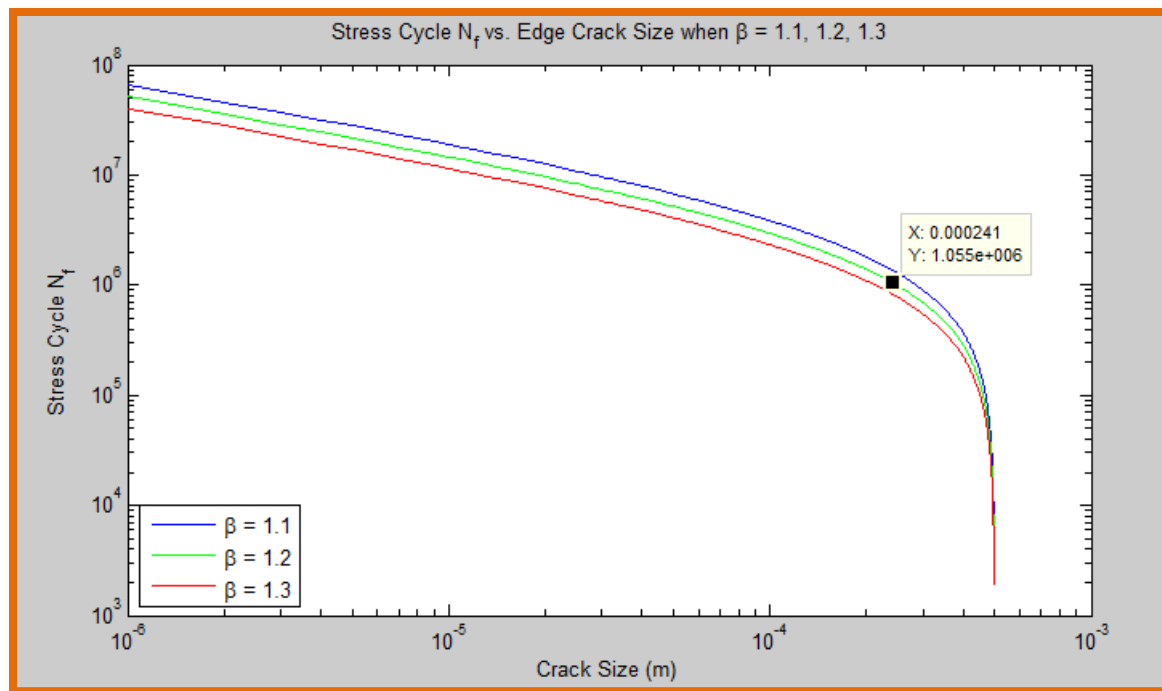


Figure 21: Stress Cycle N_f vs. Edge Crack Size.

As illustrated from Figure 21, a life cycle over 10^6 the edge crack size needs to be less than 0.2mm. At this range, the manufacturability of this material is realistic. By building the design with a crack size of smaller than 0.2mm, the connecting rod is expected to survive its lifetime operation. If later a crack size slightly larger than 0.2mm is used, the thickness b must increase accordingly. Although there won't be much change as this is already in the range of 10^6 cycles and already an optimized design. From a manufacturing standpoint

manufacturing crack sizes below 0.2mm is not a big issue. Designing this connecting rod is very realistic and as long as the crack size remains below 0.2mm, the connecting rod is safe from fracture base on Mode I.

13 SOLIDWORKS AND ABAQUS 3D DESIGN OPTIMIZATION

After finding the critical angle from Comsol, Matlab, and obtaining necessary stress and forces, these values are inputted into Solidworks and Abaqus for stress analysis and optimization. This critical step is where all the work performed previously will be integrated together for the optimization analysis.

In the optimization, the focus will be on the pocket depth and finding the optimized values that do not exceed the imposed factor of safety (FOS) 1.5. To do this optimization, a simple analysis in Solidworks will be performed first since it is more user friendly and optimized quicker. Next the same connecting rod (already or close to optimized) with different cross-section will be imported into Abaqus and optimized to verify the stress.

Recall that:

$$\text{Eq 13-1} \quad S_{\text{accepted failure}} = \frac{S_y}{FOS} = \frac{460 \text{ MPa}}{1.5} = 305 \text{ MPa}$$

In Table 13 shown below, anything in red is a stress over 305 MPa while anything in green is the critical stress optimization desired.

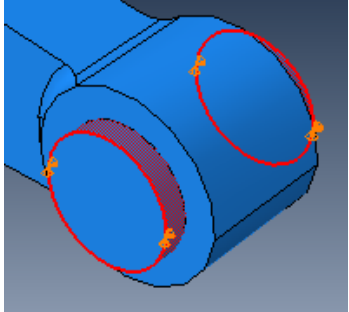
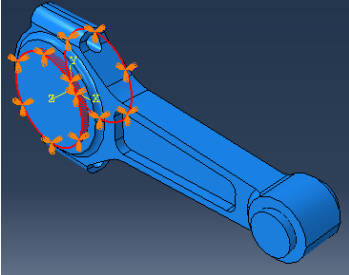
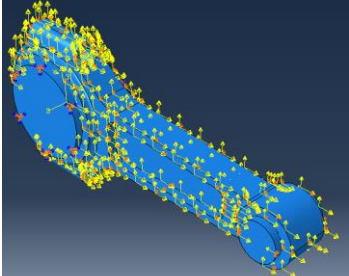
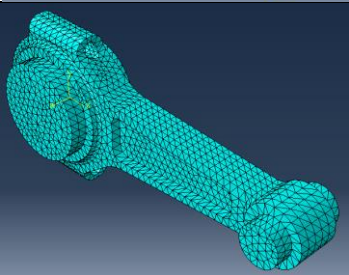
Table 13: Solidworks optimization data (For all the Stress plot look below).

Scenario	Initial	Optimized	1	2	3	4
Side Pocket Depth (m)	0.00635m	0.007915m	0.003175m	0.003965m	0.004755m	0.005545m
Stress (Pa)	2.51E+08	3.03E+08	1.74E+08	1.91E+08	2.09E+08	2.29E+08
Mass (kg)	2.68151 kg	2.62293 kg	2.80038 kg	2.7708 kg	2.74123 kg	2.71165 kg
Scenario	5	6	7	8	9	10
Side Pocket Depth (m)	0.006335m	0.007125m	0.007915m	0.008705m	0.009495m	0.009525m
Stress (Pa)	2.50E+08	2.75E+08	3.03E+08	3.41E+08	3.88E+08	3.94E+08
Mass (kg)	2.68208 kg	2.6525 kg	2.62293 kg	2.59335 kg	2.56378 kg	2.56265 kg

Note: For detail of load, fixtures, mesh control refer to the Appendix.

From Table 13, the optimized pocket depth of the connecting rod from each side is 0.007915m and optimized mass is 2.62293 kg. This model will be imported into Abaqus to perform further analysis for better results.

Table 14: Force application and boundary conditions table (Solidworks is applied in a similar so not listed here).

Conditions	Values
Prescribed displacement: $Y = 0 \text{ m}$ $Z = 0 \text{ m}$ Prescribed Body load: $X = \text{FPRa}$ $Y = 0 \text{ N}$	
Prescribed displacement fixed/anchored. No Rotation as well.	
Body load: $X = b_a \text{ N/m}^3$ $Y = b_t \text{ N/m}^3$ Eq 13-2 $b_a = -\rho(\ddot{G}_a - \ddot{\gamma}Y - \dot{\gamma}^2X)$ Eq 13-3 $b_t = -\rho(\ddot{G}_t + \ddot{\gamma}X - \dot{\gamma}^2Y)$	
Mesh size: Approximate Global Size: 0.005 Mesh type: tetrahedral (Finer mesh took longer than half hour so results was run at 0.005)	

The figure above shows the boundary and force conditions imposed on the Abaqus model for the analysis. The values and equations received for b_a and b_t are from the Matlab code.

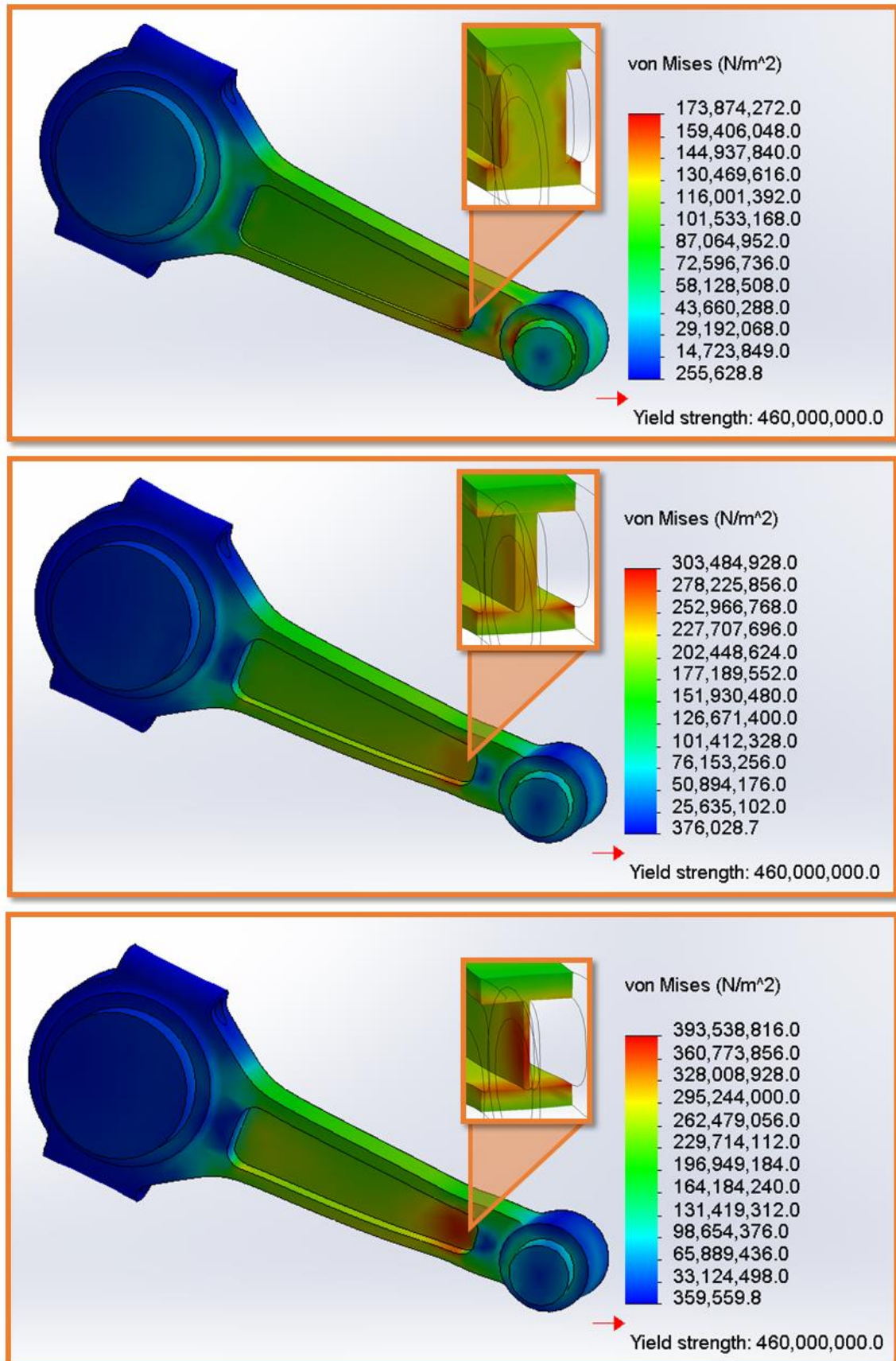


Figure 22: (Top) Pocket depth: 0.003175m (Middle) Optimized (Bottom) Pocket depth: 0.009525.

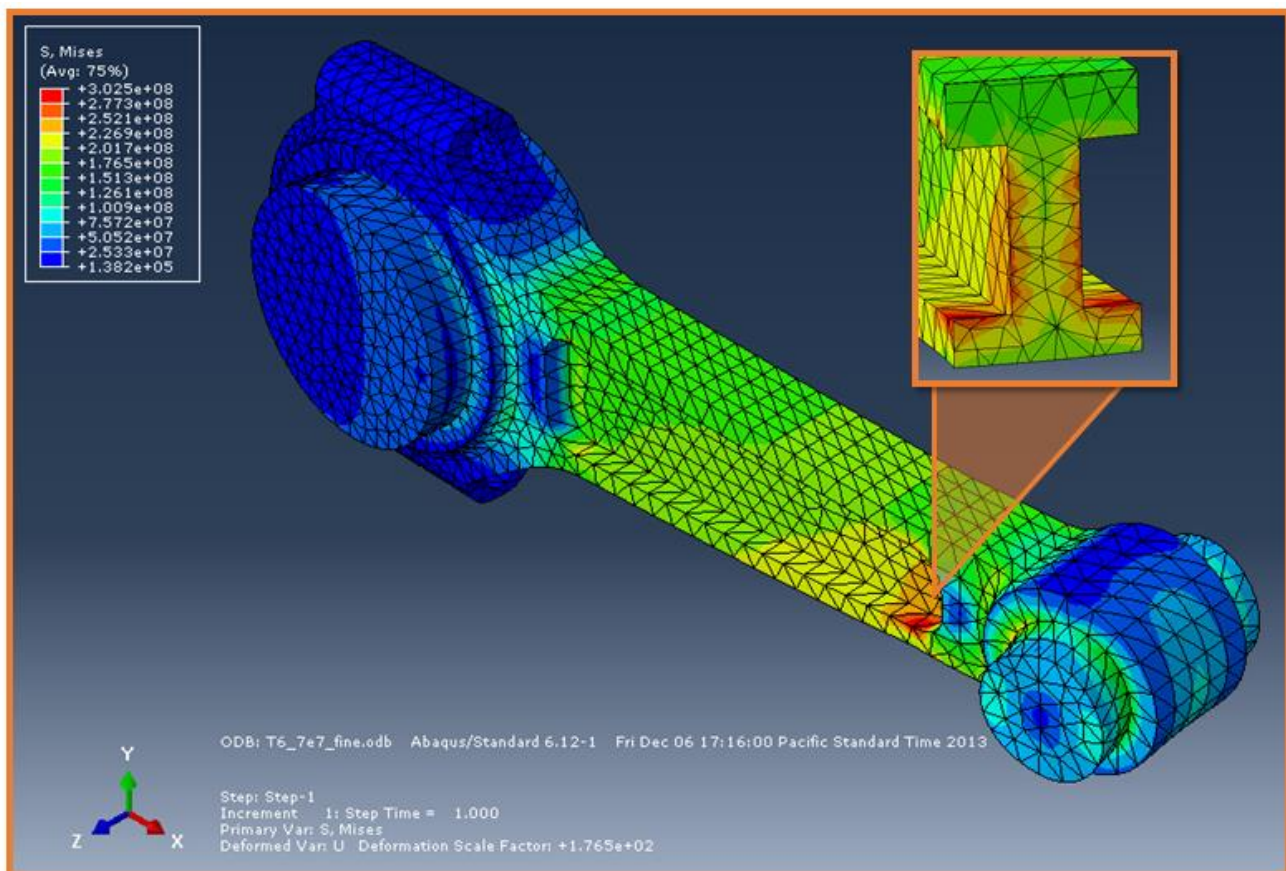
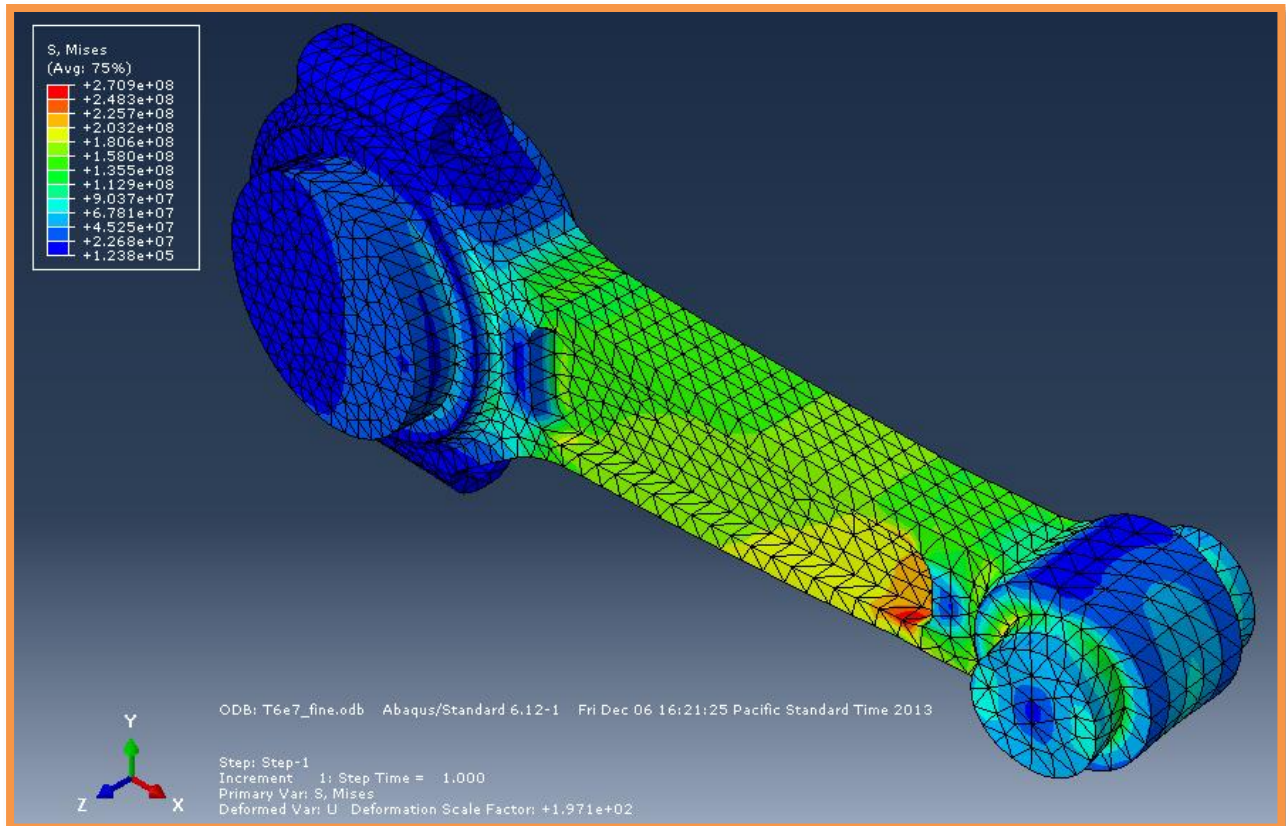


Figure 23: Tensile Stress at: (Top) Pocket depth: .007515 m (Bottom) Optimized Pocket depth: 0.007915m.

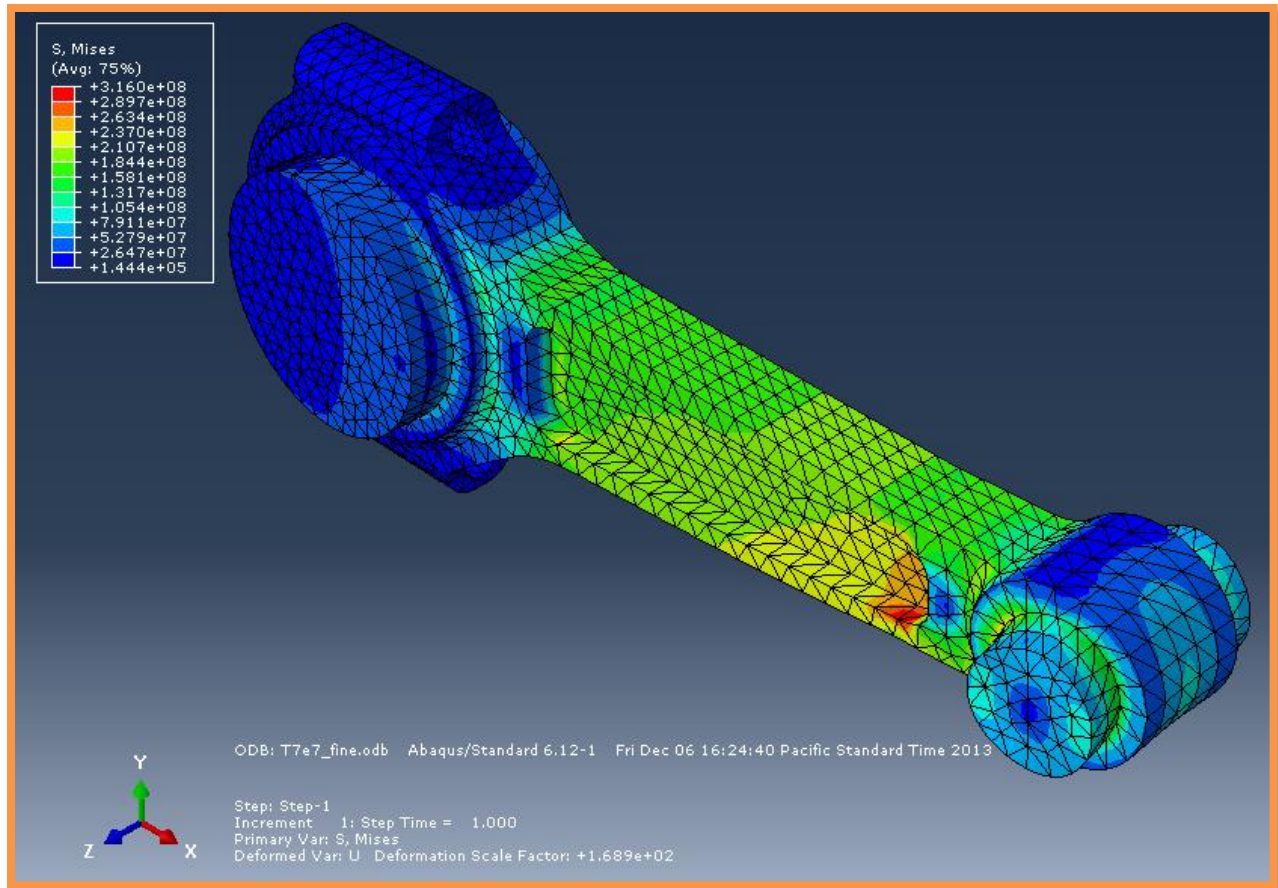


Figure 24: Tensile Stress at Pocket depth: 0.008115m.

Looking at the results above, the values closely match the one done in Solidworks at the angle of max tensile stress.

For compression, the values go much higher as shown in Figure 25 below for compression.

In the end, from the Abaqus and Solidworks optimization analysis, the smallest thickness that still satisfies the imposed factor of safety 1.5. The result obtained is the thickness 0.007915m. With this thickness, the stress can be kept below the 305MPa as shown in the Solidworks and Abaqus figure above.

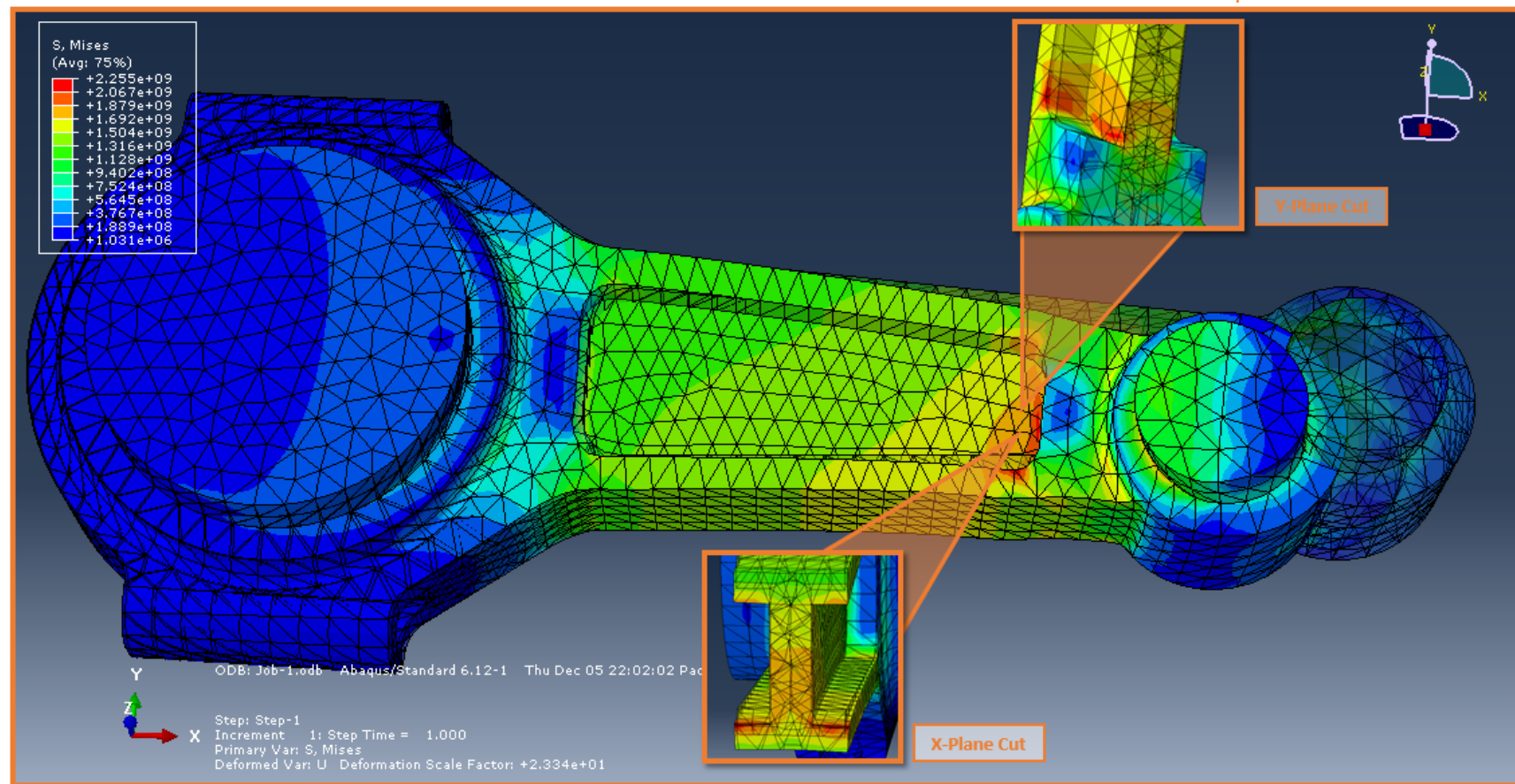


Figure 25: Compressive Stress at Pocket size: 0.007915m.

14 DISCUSSION & CONCLUSIONS

The load analysis results indicate that the maximum axial force occurs at around 0 rad when the force exerted on the connecting rod by the crankshaft and piston are at their peaks. This also means that the stress should be the highest around 0 rad as well. This data of the connecting rod is used to figure out the safety factors using MATLAB. The finite element analysis results gave a safety factor of 5.97 because the rod has a changing cross section and the larger cross section was used. This results in having a higher safety factor from MATLAB than in COMSOL. For COMSOL, a safety factor of 1.5 was determined and would be the optimal safety factor desired, which is around 1.5 to 2.5. Thus, the design should be optimized by changing the beam cross section and varying the surface area of the pin location. By changing the the beam cross section and the pin contact surface, the stresses are expected to also change at this location which would help improve the connecting rod.

Analysis is most effective when the connecting rod is in constant angular speed. During constant angular speed of 3,800 rpm, the finite element analysis results illustrate that the connecting rod is able to withstand the stresses and function normally providing 132 Nm of torque as expected. At 3,800 rpm, the maximum stress is at 305 MPa which is around 75% of the 460 MPa yield strength, and this gives a safety factor of 1.5. The finite element analysis results indicate very minimum stress in the beam column. Thus, improvements on the connecting rod can be made such as varying the thickness of the middle column to reduce mass. The middle column can be changed from a rectangular cross section to an I-beam or H-beam. We expect this change to lower the mass without compromising strength and the safety factor.

One of the assumptions made is that the engine operates at a constant 3,800 rpm. However, in reality, all the connecting rods would experience an acceleration

when the gas pedal is pressed. The assumption regarding the constant angular speed for the connecting rod would fail to include this extra inertial force that comes from the acceleration. Also, the whole car experiences linear translation during this instant, which is not incorporated into the final design estimation. Moreover, thermal expansion, electromagnetic, and extraneous effects that may change material properties and therefore induce forces are also mostly ignored. Further analysis and optimization should be done on the connecting rod to incorporate these factors.

From the final optimization analysis, a safe connecting rod with a safety factor of ~ 1.5 can be designed if the thickness of the pocket depth is reduced down to 0.007915m. As long as that is used, the connecting rod made of Steel 4310 is expected to have infinite life through the fatigue analysis. This is because with 25,000 miles the engine already experienced infinite life base collected data. So to survive 200,000 miles, the engine must definitely be in the infinite life range. The results were not too surprising as the connecting rod is expected to have infinite life based on the initial hypothesis before the calculations. As for fracture, using Mode I and a crack size below 0.2mm when manufactured, the connecting rod survives for an infinite cycles (refer back to Stress Cycle N_f vs. Crack Size plot for more details).

15 SUMMARY AND CONCLUSIONS

The preliminary model for a connecting rod used in a Toyota 1NR-FE 4-cylinder engine was designed. 4130 Steel was selected as the material for the connecting rod due to its high strength and long fatigue life. An initial rectangular cross section was used to simulate the connecting rod for simplicity and quick stress and safety factor calculations. The connecting rod is assumed to undergo constant angular speed of 3,800 rpm, at which the maximum stress was determined to be 305 MPa. This is around 75% of the material yield strength

which is 460 MPa, and gives a safety factor of 1.5. Using 4130 Steel, the connecting rod lasts infinite fatigue life, withstanding 8.33×10^6 Engine Stress Cycles and 200,000 miles. And as for fracture, using Mode I with a crack size below 0.2mm when manufactured, the connecting rod survives for infinite cycles.

16 ACKNOWLEDGEMENTS

We would like to acknowledge Professor Ghoniem and TA Andrew Sheng for their help.

17 REFERENCES

- [1] "The Four Stroke Engine Connecting Rod." *The Four Stroke Engine Connecting Rod*. N.p., n.d. Web. 30 Oct. 2013.
- [2] "Connecting Rods 101 Design,Material,Modifications,and Machining." *DSM Forums RSS*. N.p., n.d. Web. 30 Oct. 2013.
- [3] Po, Giacomo, Nasr Ghoniem and Daniel Welch. "Damage and Failure of Materials in Mechanical Design." 2012. Document. 10 October 2013.
- [4] Tan, Paul. *Toyota Auris gets new Toyota 1NR-FE 1.33L Dual VVT-i engine in UK line-up*. 19 November 2008. 15 October 2013.
<<http://paultan.org/2008/11/19/toyota-auris-gets-new-toyota-1nr-fe-133l-dual-vvt-i-engine-in-uk-line-up/>>.
- [5] "TOYOTA AURIS TECHNICAL SPECIFICATIONS." *TOYOTA OPTIMAL DRIVE 1.33 DUAL VVT-i*. n.d. Document. 23 January 2013.
<http://media.toyota.co.uk/wp-content/files_mf/1329495406120216MTOYOTAAURISTECHNICALSPECIFICATIONS.pdf>. - (added to reference pg for quick reference.)
- [6] Budynas, Richard G. and J. Keith Nisbett. "Shigley's Mechanical Engineering Design." *9th Edition*. McGraw-Hill, 2011. Textbook.

18 APPENDICES

18.1 *Kinematic Equations Derivations*

Eq 18-1

$$\begin{aligned}\sin(\gamma) &= \lambda \sin(\Theta) \\ \gamma' \cos(\gamma) &= \lambda \Theta' \cos(\Theta) \\ \gamma' &= \omega \lambda \cos(\Theta) / \cos(\gamma) A = \pi r^2\end{aligned}$$

note:

let $\Theta = \varphi$

$$\sin^2(\gamma) + \cos^2(\gamma) = 1$$

$$\cos(\gamma) = (1 - \sin^2(\gamma))^{0.5}$$

$$\cos(\gamma) = [1 - (\lambda \sin(\Theta))^2]^{0.5}$$

$$(1): \gamma' = \omega \lambda \cos(\Theta) / [1 - \lambda^2 \sin^2(\Theta)]^{0.5}$$

Eq 18-2

$$\begin{aligned}\text{From (1): } \gamma' [1 - \lambda^2 \sin^2(\Theta)]^{0.5} &= \omega \lambda \cos(\Theta) \\ \gamma'' [1 - \lambda^2 \sin^2(\Theta)]^{0.5} + 0.5 \gamma' [1 - \lambda^2 \sin^2(\Theta)]^{-0.5} \cdot \Theta' (2\lambda^2 \sin(\Theta) \cos(\Theta)) &= \omega' \lambda \cos(\Theta) - \Theta' \omega \lambda \sin(\Theta)\end{aligned}$$

note:

$$\omega' = 0$$

$$(1): \gamma' = \omega \lambda \cos(\Theta) / [1 - \lambda^2 \sin^2(\Theta)]^{0.5}$$

$$\begin{aligned}\gamma'' [1 - \lambda^2 \sin^2(\Theta)]^{0.5} + \{ \omega \lambda \cos(\Theta) / [1 - \lambda^2 \sin^2(\Theta)]^{0.5} \} \cdot \{ \omega \lambda^2 \sin(\Theta) \cos(\Theta) / [1 - \lambda^2 \sin^2(\Theta)]^{0.5} \} &= \omega^2 \lambda \sin(\Theta) \\ \gamma'' [1 - \lambda^2 \sin^2(\Theta)]^{0.5} + \omega^2 \lambda^2 \cos^2(\Theta) \sin(\Theta) / (1 - \lambda^2 \sin^2(\Theta)) &= [\omega^2 \lambda \sin^2(\Theta) - \omega^2 \lambda^3 \sin^3(\Theta)] / (1 - \lambda^2 \sin^2(\Theta)) \\ \gamma'' [1 - \lambda^2 \sin^2(\Theta)]^{0.5} &= \{ \omega^2 \lambda \sin(\Theta) - \omega^2 \lambda^3 \sin(\Theta) [\sin^2(\Theta) + \cos^2(\Theta)] \} / (1 - \lambda^2 \sin^2(\Theta))\end{aligned}$$

note:

$$\sin^2(\Theta) + \cos^2(\Theta) = 1$$

$$(2): \gamma'' = \omega^2 \lambda \sin(\Theta) [1 - \lambda^2] / [1 - \lambda^2 \sin^2(\Theta)]^{3/2}$$

Eq 18-3

$$\begin{aligned}\mathbf{R} &= -r \sin(\Theta) \hat{\mathbf{i}} + r \cos(\Theta) \hat{\mathbf{j}} \\ \mathbf{R}' &= -r \Theta' \cos(\Theta) \hat{\mathbf{i}} - r \Theta' \sin(\Theta) \hat{\mathbf{j}} \\ \mathbf{R}'' &= -r \Theta'' \cos(\Theta) \hat{\mathbf{i}} + r \Theta'^2 \sin(\Theta) \hat{\mathbf{i}} - r \Theta'' \sin(\Theta) \hat{\mathbf{j}} - r \Theta'^2 \cos(\Theta) \hat{\mathbf{j}}\end{aligned}$$

note:

$$\Theta' = \omega$$

$$\Theta'' = 0 \text{ because constant angular speed } \omega$$

$$\mathbf{R}'' = \omega^2 (r \sin(\Theta) \hat{\mathbf{i}} - r \cos(\Theta) \hat{\mathbf{j}})$$

note:

$$\mathbf{R} = -r \sin(\Theta) \hat{\mathbf{i}} + r \cos(\Theta) \hat{\mathbf{j}}$$

$$(3): \mathbf{R}'' = -\omega^2 \mathbf{R}$$

Eq 18-4

$$\mathbf{P} = [r \cos(\Theta) - \ell \cos(\gamma)] \hat{\mathbf{j}}$$

$$\mathbf{P} = \ell [\lambda \cos(\Theta) - \cos(\gamma)] \hat{\mathbf{j}}$$

$$\mathbf{P}' = \ell [-\lambda \Theta' \sin(\Theta) + \gamma' \sin(\gamma)] \hat{\mathbf{j}}$$

note:

$$\sin(\gamma) = \lambda \sin(\Theta)$$

$$\mathbf{P}' = \ell [-\lambda \Theta' \sin(\Theta) + \gamma' \lambda \sin(\Theta)] \hat{\mathbf{j}}$$

$$\mathbf{P}'' = \ell [-\lambda \Theta'' \sin(\Theta) - \lambda \Theta'^2 \cos(\Theta) + \gamma'' \lambda \sin(\Theta) + \gamma' \Theta' \lambda \cos(\Theta)] \hat{\mathbf{j}}$$

note:

$$\Theta' = \omega$$

$$\Theta'' = 0 \text{ because constant angular speed } \omega$$

$$\mathbf{P}'' = \ell [-\lambda \omega^2 \cos(\Theta) + \gamma'' \lambda \sin(\Theta) + \gamma' \omega \lambda \cos(\Theta)] \hat{\mathbf{j}}$$

$$\mathbf{P}'' = \ell \lambda [-\omega^2 \cos(\Theta) + \gamma'' \sin(\Theta) + \gamma' \omega \cos(\Theta)] \hat{\mathbf{j}}$$

$$(4) \mathbf{P}'' = \ell \lambda [(\gamma' - \omega) \omega \cos(\Theta) + \gamma'' \sin(\Theta)] \hat{\mathbf{j}}$$

Eq 18-5

$$\mathbf{G} = \mathbf{R} + \beta(\mathbf{P} - \mathbf{R})$$

$$\mathbf{G} = (1 - \beta)\mathbf{R} + \beta\mathbf{P}$$

$$\mathbf{G}' = (1 - \beta)\mathbf{R}' + \beta\mathbf{P}'$$

$$(5) \mathbf{G}'' = (1 - \beta)\mathbf{R}'' + \beta\mathbf{P}''$$

18.2 Force Components in the Inertial Reference Frame derivations

Eq 18-6

$$m_P \mathbf{P}'' = -p(\theta)A \hat{\mathbf{j}} - \Phi_{PR} + \Phi_{CP} \hat{\mathbf{i}}$$

$$m_P \mathbf{P}''_y = -p(\theta)A - \Phi_{PRy}$$

$$(6) \Phi_{PRy} = -m_P \mathbf{P}''_y - p(\theta)A$$

Eq 18-7

$$m_G \mathbf{G}'' = \Phi_{PR} + \Phi_{SR}$$

$$m_G \mathbf{G}''_y = \Phi_{PRy} + \Phi_{SRy}$$

$$(7) \Phi_{SRy} = m_G \mathbf{G}''_y - \Phi_{PRy}$$

Eq 18-8

$$J_G \gamma'' = \Phi_{PR} \times (G \cdot P) + \Phi_{SR} \times (G \cdot R)$$

$$J_G \gamma'' = (\Phi_{PR} \hat{i} + \Phi_{PR} \hat{j}) \times [(\beta-1)(-R_x) \hat{i} + (\beta-1)(P_y - R_y) \hat{j}] + (\Phi_{SR} \hat{i} + \Phi_{SR} \hat{j}) \times [\beta R_x \hat{i} + \beta(P_y - R_y) \hat{j}]$$

$$J_G \gamma'' = (\beta-1)\Phi_{PRx}(P_y - R_y) + (\beta-1)\Phi_{PRy}R_x + \beta\Phi_{SRx}(P_y - R_y) + \beta\Phi_{SRy}R_x$$

note: substitute (9) $\Phi_{SRx} = m_G G_x'' - \Phi_{PRx}$

$$J_G \gamma'' = (\beta-1)\Phi_{PRx}(P_y - R_y) + (\beta-1)\Phi_{PRy}R_x + \beta(m_G G_x'' - \Phi_{PRx})(P_y - R_y) + \beta\Phi_{SRy}R_x$$

$$-(\beta-1)\Phi_{PRx}(P_y - R_y) + \beta\Phi_{PRx}(P_y - R_y) = -J_G \gamma'' + (\beta-1)\Phi_{PRy}R_x + \beta m_G G_x''(P_y - R_y) + \beta\Phi_{SRy}R_x$$

$$\Phi_{PRx}(P_y - R_y) = -J_G \gamma'' + (\beta-1)\Phi_{PRy}R_x + \beta m_G G_x''(P_y - R_y) + \beta\Phi_{SRy}R_x$$

$$\boxed{(8) \Phi_{PRx} = \beta m_G G_x'' - \{[J_G \gamma'' - ((\beta-1)\Phi_{PRy} + \beta\Phi_{SRy})R_x] / (P_y - R_y)\}}$$

Eq 18-9

$$m_G G'' = \Phi_{PR} + \Phi_{SR}$$

$$m_G G_x'' = \Phi_{PRx} + \Phi_{SRx}$$

$$\boxed{(9) \Phi_{SRx} = m_G G_x'' - \Phi_{PRx}}$$

18.3 *Materials Properties*

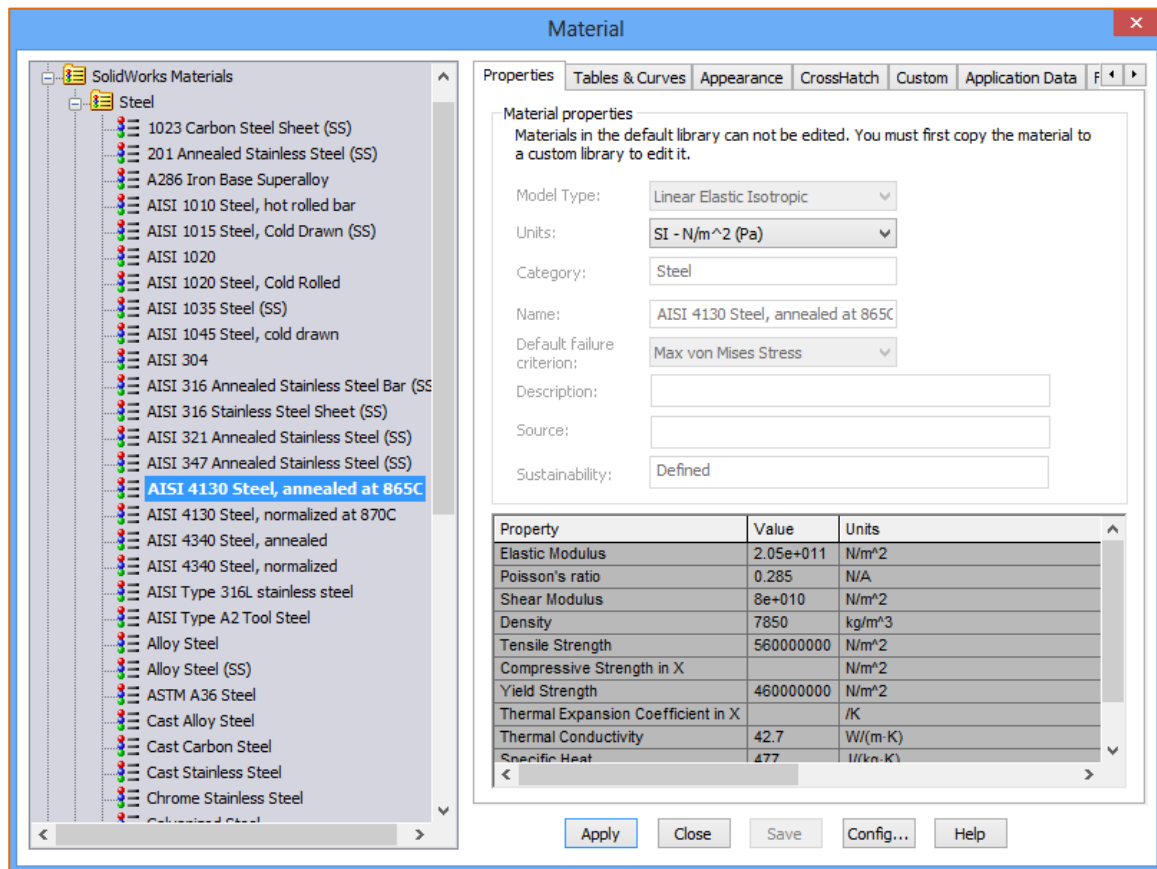


Figure 26: Material properties of the connecting rod.

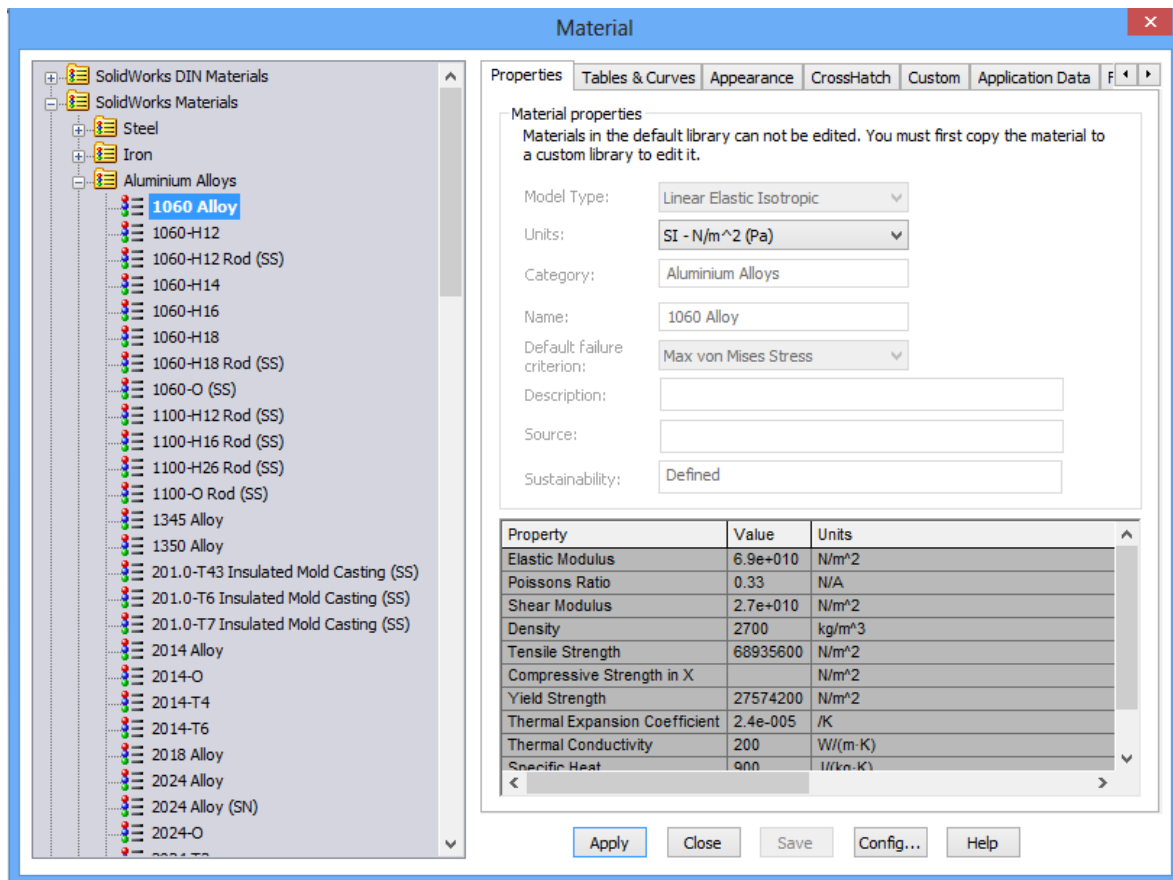


Figure 27: Failed material properties of the connecting rod.

18.4 TOYOTA AURIS TECHNICAL SPECIFICATIONS

[5] Check Reference for full details

TOYOTA OPTIMAL DRIVE 1.33 DUAL VVT-i					
Engine Code		1NR-FE			
Type		Four cylinders in-line			
Valve mechanism		DOHC 16-valve			
Displacement (cc)		1,329			
Bore x stroke (mm)		72.5 x 80.5			
Compression ratio		11.5 : 1			
Max power (bhp @ rpm)		100 @ 6,000			
Max torque (Nm @ rpm)		132 @ 3,800			
TOYOTA OPTIMAL DRIVE 1.6 VALVEMATIC					
Engine Code		1ZR-FAE			
Type		Four cylinders in-line			
Valve mechanism		DOHC 16-valve Valvematic			
Displacement (cc)		1,598			
Bore x stroke (mm)		80.5 x 78.5			
Compression ratio		10.7 : 1			
Max power (bhp @ rpm)		130 @ 6,400			
Max torque (Nm @ rpm)		160 @ 4,400			
TOYOTA OPTIMAL DRIVE 1.4 D-4D DPF					
Engine Code		1ND-TV			
Type		Four cylinders in-line			
Valve mechanism		DOHC 8-valve			
Displacement (cc)		1,364			
Bore x stroke (mm)		73.0 x 81.5			
Compression ratio		16.5 : 1			
Max power (bhp @ rpm)		89 @ 3,800			
Max torque (Nm @ rpm)		205 @ 3,000			
TRANSMISSIONS	1.33 DUAL VVT-i	1.6 VALVEMATIC	1.4 D-4D DPF		
Type	Single dry plate				
Gear Ratios					
1 st	3.538	3.538	3.538		
2 nd	1.913	1.913	1.913		
3 rd	1.310	1.310	1.310		
4 th	0.971	0.971	0.971		
5 th	0.818	0.818	0.714		
6 th	0.700	0.700	0.619		
Reverse	3.333	3.333	3.333		
Differential gear ratio					
Differential gear ratio	4.562	4.562	3.944	3.944	3.944

PERFORMANCE	1.33 DUAL VVT-i	1.6 VAL VEMATIC		1.4 D4D DPF	
Transmission	6 M/T	6M/T	M/M	6M/T	M/M
Max Speed (mph)	109	121	121	109	109
0-62mph (sec)	13.1	10.0	11.9	11.9	12.0
Fuel consumption					
Combined	48.7	42.8	44.8	58.9	57.6
Extra-urban	55.4	51.4	52.3	65.7	64.2
Urban	39.8	32.8	35.3	49.6	48.7
Tank capacity (l)	55				

EMISSIONS, VED & INSURANCE	1.33 DUAL VVT-i	1.6 VALVEMATIC		1.4 D-4D DPF	
Transmission	6 M/T	6M/T	M/M	6M/T	M/M
Combined	135 (TR 136)	153 (SR 154)	146	128	130
Extra-urban	118 (TR 119)	127 (SR 128)	125	114	116
Urban	165 (TR 165)	198 (SR 198)	184	152	154
VED Band	E	G	F	D	D
Insurance groups	10E to 16E				
BRAKES	1.33 DUAL VVT-i	1.6 VALVEMATIC		1.4 D-4D	
Front (mm)	Ventilated discs ø273 x 26				
Rear (mm)	Solid discs ø270 x 10				
Additional features	A BS, EBD, BA. Opt: VSC, TRC				
ABS = anti-lock br aking system – EBD = electronic brakeforce distribution – BA = brake assist VSC+ = vehicle st ability control plus – TRC = traction control – HAC = hill start assist control					
SUSPENSION					
Front		L-arm MacPherson strut			
Rear		Torsion beam			
STEERING					
Type		Rack and pinion, Electric Power Steering			
Ratio		14.42:1 (1.6 manual 14.44:1)			
Turns lock-to-lock		2.9			
Min turning radius – t yre (m)		5.2			
EXTERIOR DIMENSI ONS					
Overall length (mm)		4,245			
Overall width (mm)		1,760			
Overall height (mm)		1,515 (SR 1,505)			
Wheelbase (mm)		2,600			
Front track (mm)		1,536 (15in wheel)			

Rear track (mm)		1,533 – 1,535			
Front overhang (mm)		905			
Rear overhang (mm)		745			
Drag coefficient (Cd)		0.29			
INTERIOR DIMENSIONS					
Interior length (mm)		1,985			
Interior width (mm)		1,460			
Interior height (mm)		1,245			
VDA Capacity, (rear seats up) (l)		354			
VDA Capacity, (rear seats down) (l)		761			
WEIGHTS (kg)	1.33 DUAL VVT-i	1.6 VALVEMATIC		1.4 D-4D 90	
Kerb weight	1,280 - 1,285	1,275 – 1,315	1,280 – 1,320	1,280 – 1,310	1,285 – 1,315
Gross vehicle weight	1,720	1,750	1,750	1,760	1,760
Towing capacity - braked	1,000	1,300	1,200	1,000	1,000
Towing capacity – unbraked	450	450	450	450	450

18.5 N_f cycle vs. Edge Crack Size Matlab Code

```

%+=====+%
%| Wilson Plot Data For Crack Propagation |%
%| MAE 296A Fall 2013 Graduate Course    |%
%| No reproduction in part/whole without |%
%| prior consents from author            |%
%| Author: Wilson Lam                    |%
%+=====+%
clear all;
close all;
clc;
% Constants %
B = [1.1,1.2,1.3];% Beta value is small b/c size of a is extremely small
compare to b
dO = 82.591%3.047e2;% Change in Stress (MPa)
C = 6.89e-12;% Empirical Material Constants
m = 3;% Empirical Material Constants

%% Edge Crack Size
% syms a B dO C
% Paris Equation in LEFM conditions (For assumption check MS doc.)
% Nf = (1/C)*int(1/(B*dO*(pi*a)^.5)^m,a)
% pretty(Nf)

% After integrating for Nf above subtract the Nf_final from Nf_initial
% to obtain the following Stress Cycle vs. Crack Size plot.
final = .0005;
b = 1e-6:1e-6:final;
% Nf_i=-2/(B^3*C*pi^(3/2)*a^(1/2)*dO^3) % obtain from Nf equation above.

```

```

%B = 1.1
Nf_i1=-2./(B(1)^3*C*pi^(3/2)*b.^(1/2)*dO^3);
Nf_f1=-2./(B(1)^3*C*pi^(3/2)*final^(1/2)*dO^3);
%B = 1.2
Nf_i2=-2./(B(2)^3*C*pi^(3/2)*b.^(1/2)*dO^3);
Nf_f2=-2./(B(2)^3*C*pi^(3/2)*final^(1/2)*dO^3);
%B = 1.3
Nf_i3=-2./(B(3)^3*C*pi^(3/2)*b.^(1/2)*dO^3);
Nf_f3=-2./(B(3)^3*C*pi^(3/2)*final^(1/2)*dO^3);

loglog(b,Nf_f1-Nf_i1,'b',b,Nf_f2-Nf_i2,'g',b,Nf_f3-Nf_i3,'r');
title('Stress Cycle N_f vs. Edge Crack Size when \beta = 1.1, 1.2, 1.3')
xlabel('Crack Size (m)'); ylabel('Stress Cycle N_f')
legend('\beta = 1.1', '\beta = 1.2', '\beta = 1.3',3)

```